

# Remote Monitoring of Growth and Pigmentation in Algal Cultures

A. M Collins<sup>1</sup>, T. A. Reichardt<sup>2</sup>, R. C. McBride<sup>3</sup>  
C. A. Behnke<sup>3</sup>, and J. A. Timlin<sup>1</sup>

1. Bioenergy and Defense Technology Dept., Sandia National Laboratories, Albuquerque, NM
2. Remote Sensing and Energetic Materials Dept., Sandia National Laboratories, Livermore, CA
3. Sapphire Energy, San Diego, CA

Supported by the U. S. DOE's Office of Energy Efficiency and Renewable Energy (DOE/EERE)



# Algae and the U. S. DOE

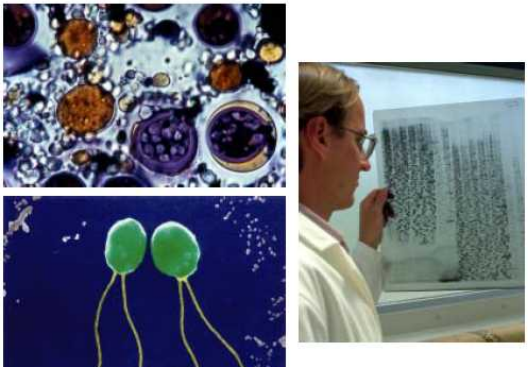
---

## 1978-1996

National Renewable Energy Laboratory 

NREL/TP-580-24190

A Look Back at the  
U.S. Department of Energy's  
Aquatic Species Program:  
Biodiesel from Algae



*Close-Out Report*

## 2010-future

U.S. DEPARTMENT OF  
**ENERGY** | Energy Efficiency &  
Renewable Energy

**BIOMASS PROGRAM**

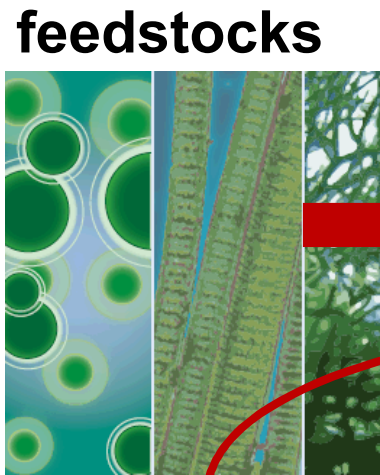


**National Algal Biofuels  
Technology Roadmap**

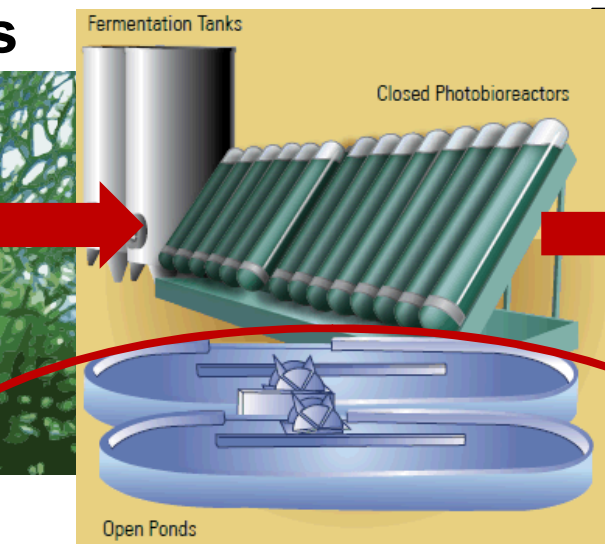
MAY 2010

# From Algae to Fuel

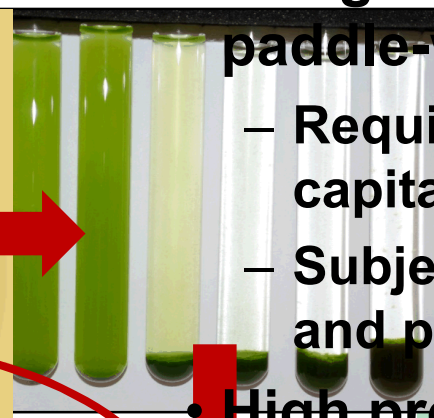
Algae  
feedstocks



Cultivation



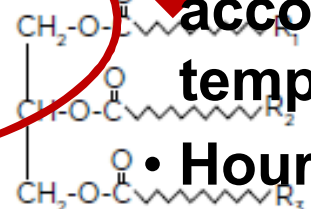
Extraction



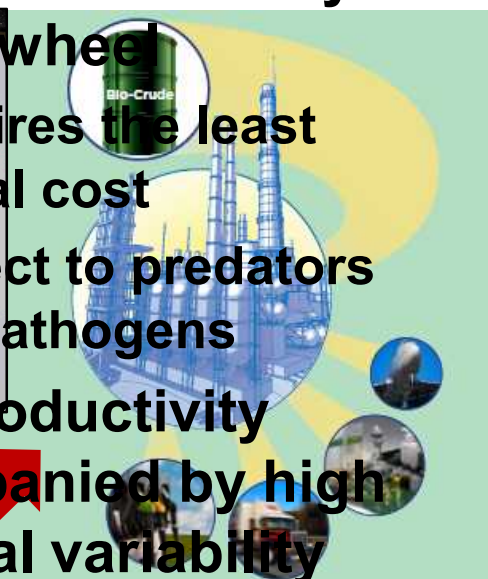
- Typically a raceway  
design regulated by a  
paddle-wheel

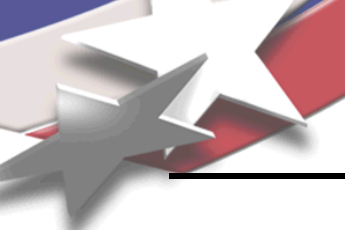
- Requires the least  
capital cost
- Subject to predators  
and pathogens

- High productivity  
accompanied by high  
temporal variability

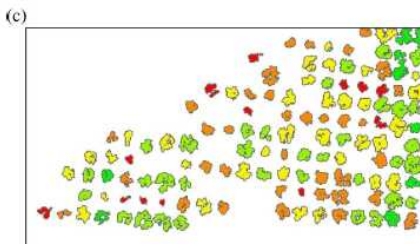
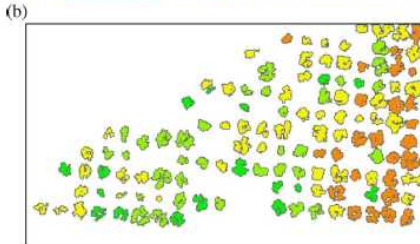


- Hours versus days

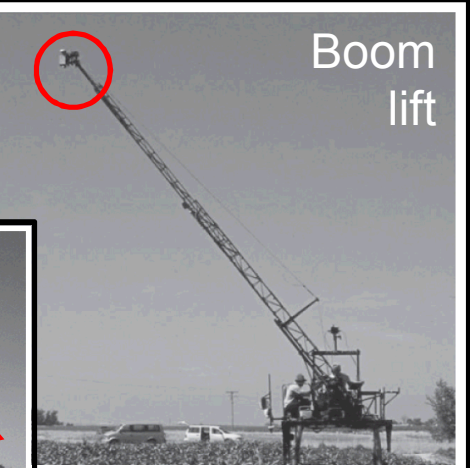
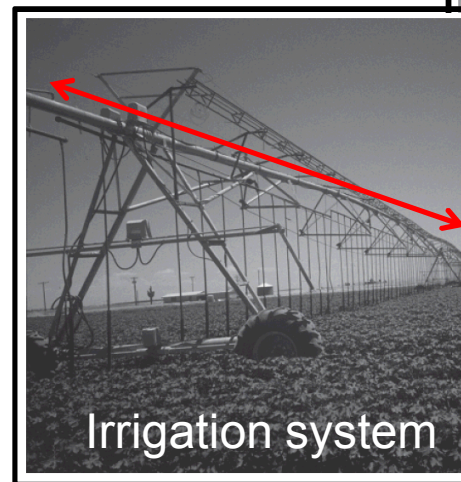




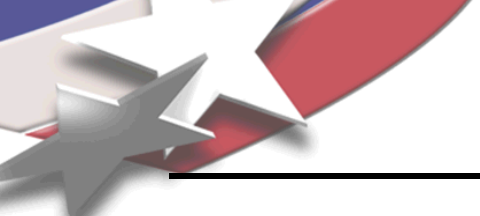
# Rapid, broad-area assessment of growth and conditions in open systems



J. A. J. Berni et al, IEEE Trans.  
Geosci .& Rem. Sens. **47**, 2009.



S. Moran et al.,  
Photogrammetric Eng. &  
Rem. Sens., June 2003,  
705-718.



# Aquaculture Pond Monitoring

---

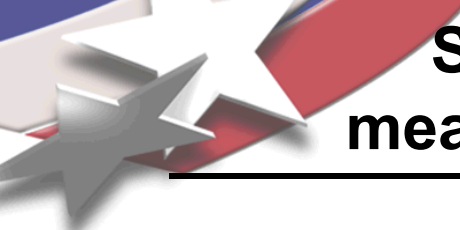
- **A. Gitelson et al. (Ben-Gurion Univ. of the Negev)**

- “Optical properties of dense algal cultures outdoors and their application to remote estimation of biomass and pigment concentration in *Spirulina platensis* (cyanobacteria),” *J. Phycol.* **31** (1995).
- “Quantitative near-surface remote sensing of wastewater quality in oxidation ponds and reservoirs: a case study,” *Water Environ. Res.* **69** (1997).
- “Comparative reflectance properties of algal cultures with manipulated densities,” *J. Appl. Phycol.* **11** (1999).
- “Optical characteristics of the phototroph *Thiocapsa roseopericina* and implications for real-time monitoring of the bacteriochlorophyll concentration,” *Appl. & Environ. Microbiology*, **65**, (1999).
- “Optical properties of *Nannochloropsis* sp and their application to remote estimation of call mass,” *Biotech. & Bioeng.* **69** (2000).

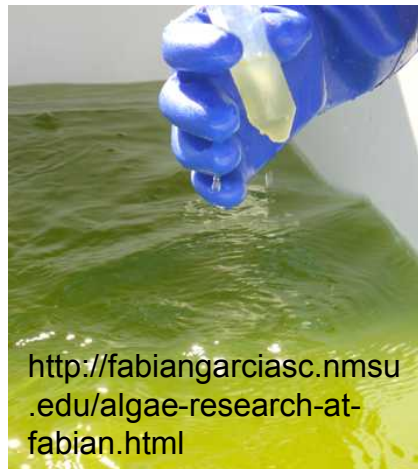
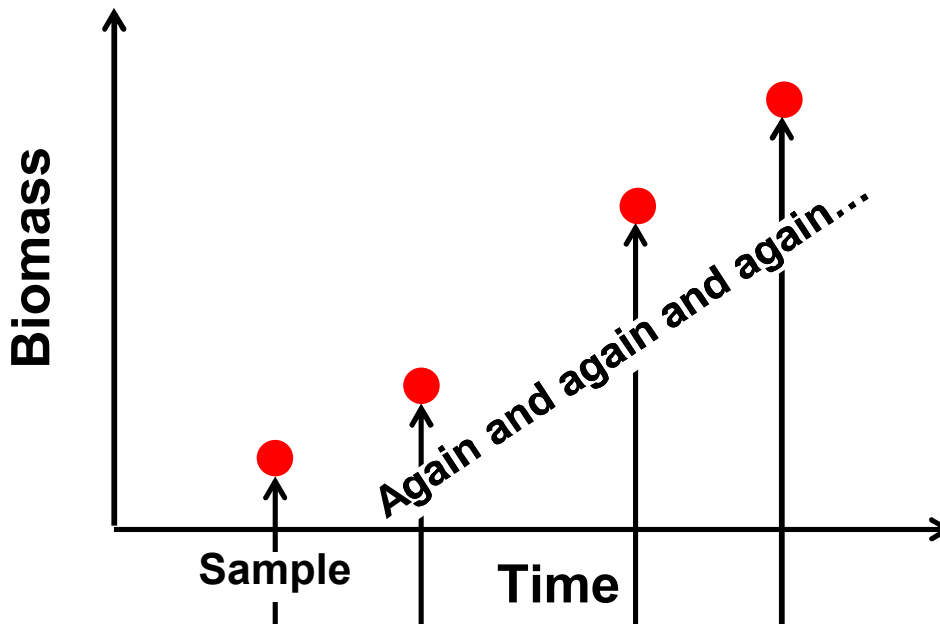
- **Recent demonstration by group at Univ. of Florida (Gainesville/Wimauma)**

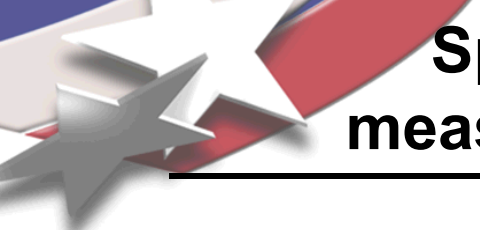


A. Abd-Elrahman et al., IPRS  
Journal of Photogrammetry  
and Remote Sensing 66,  
463-472 (2011).



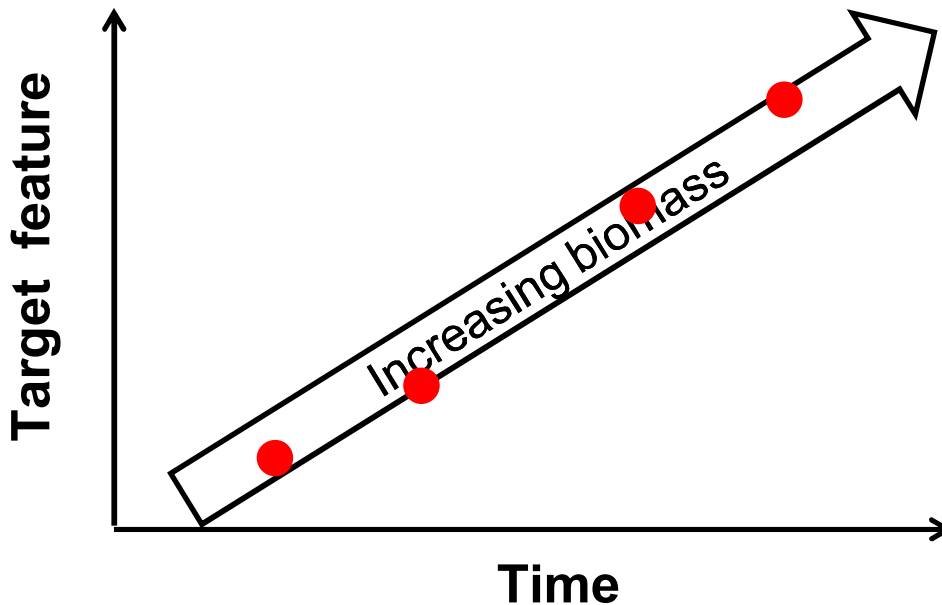
# Specific question: Can biomass be measured without sampling the culture?





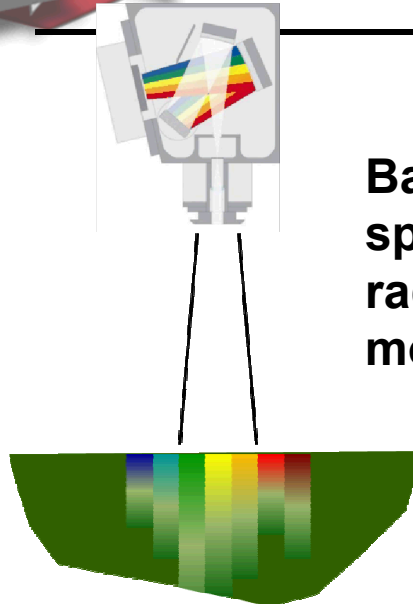
# Specific question: Can biomass be measured without sampling the culture?

---



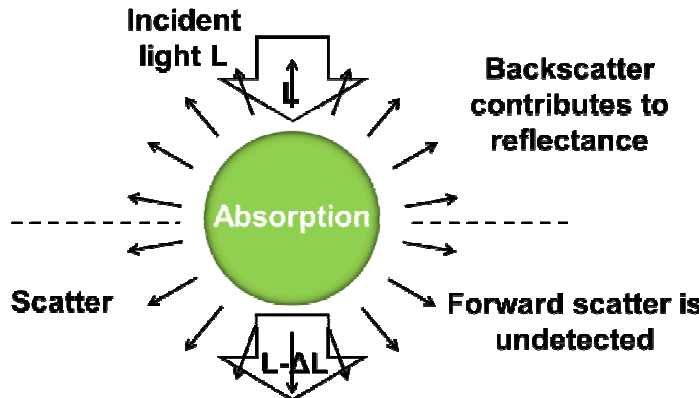
- Target feature based on collection of light
- Change in feature requires change in optical properties
- 3 effects: scattering, absorption, and re-emission (fluorescence)

# Discussion Topics



## Basics of spectro-radiometric monitoring

## Reflectance model to extract culture properties from data



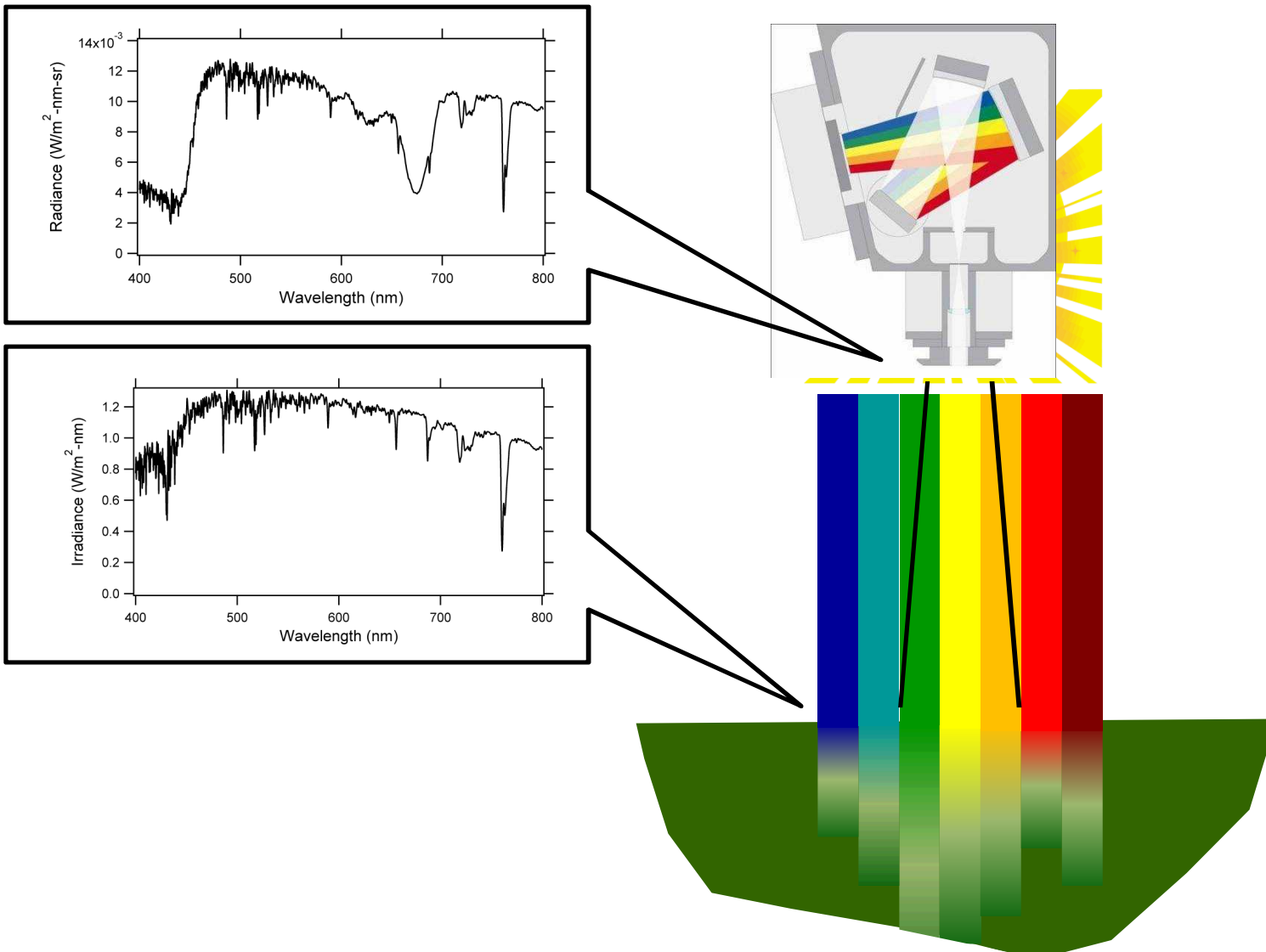
## Benchtop-scale reflectivity measurements



## Field deployment at Sapphire Energy



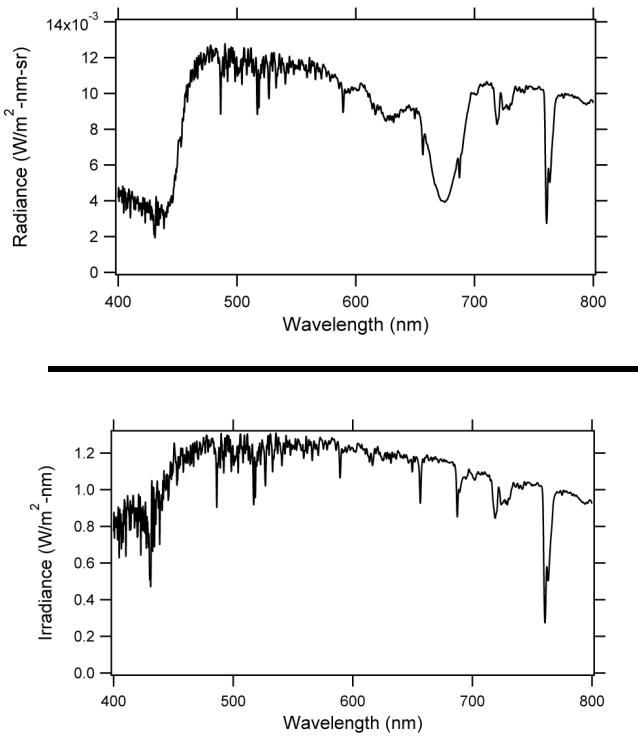
# Spectroradiometric Monitoring



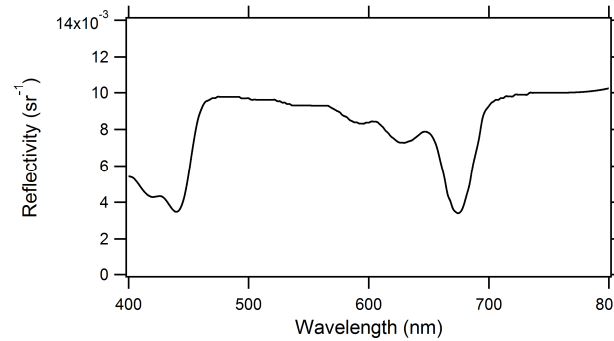


# Spectroradiometric Monitoring

---

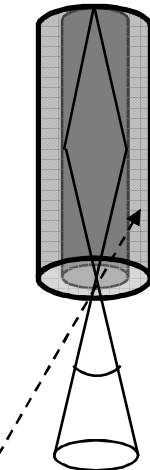
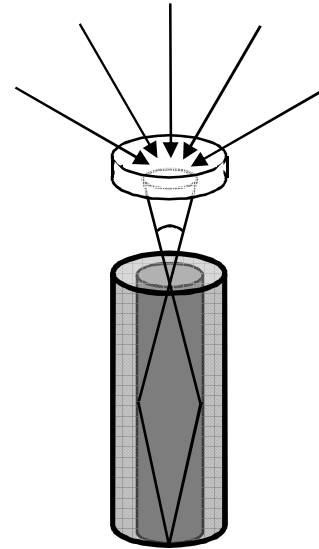


=



# Dual-Channel Spectroradiometer

- Diffuser randomizes the direction of incoming light
- Fiber captures light from all downwelling angles



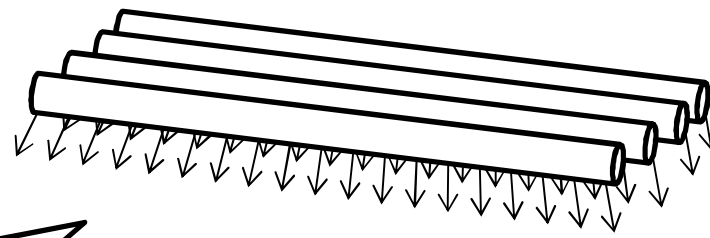
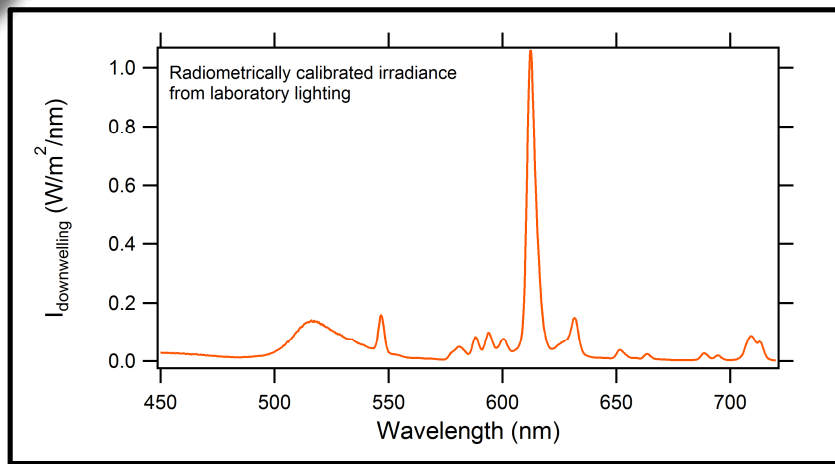
- Refractive indices of core and cladding limit field-of-view to 25° cone of light

Trapped by core

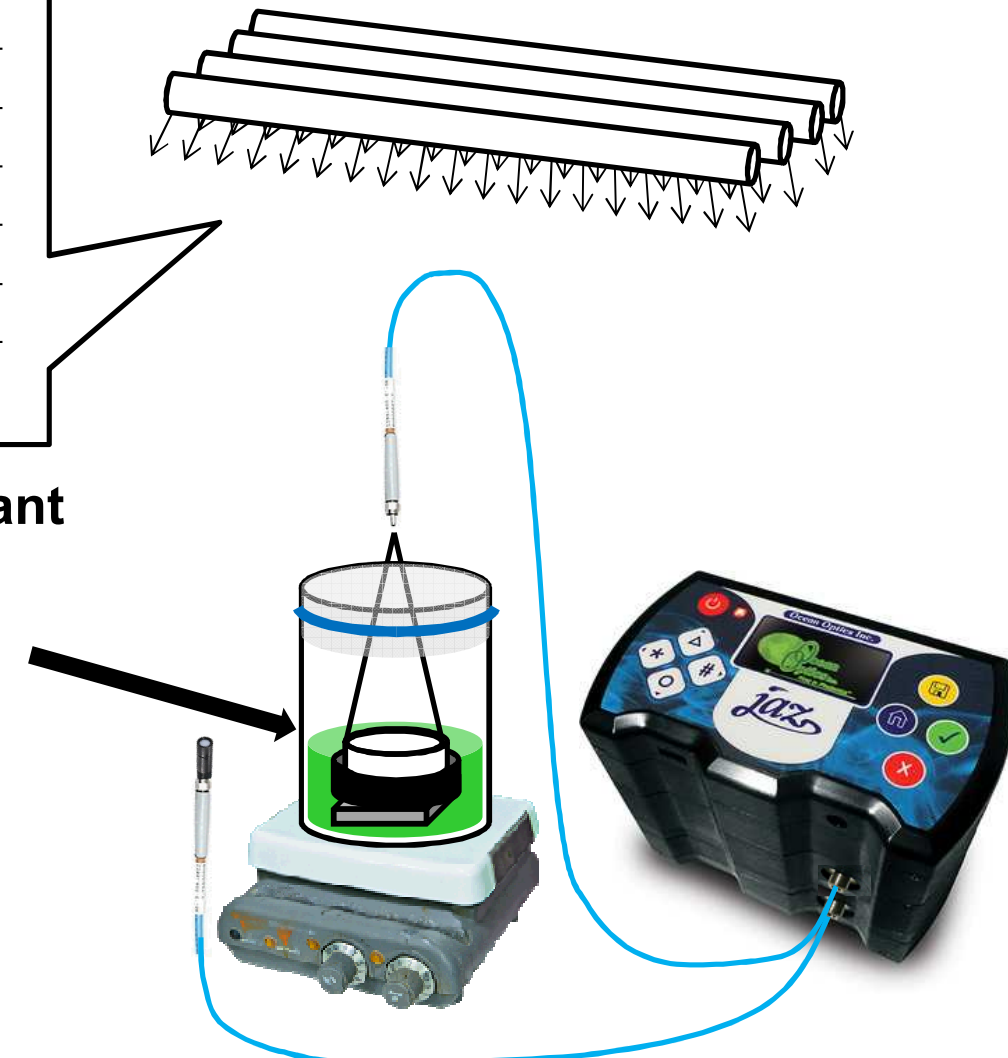
Escapes into cladding



# Benchtop-scale reflectivity measurements



- **Fluorescent lamp has significant spectral structure**
- **Algae replaced with calibrated target for absolute reflectivity measurements**

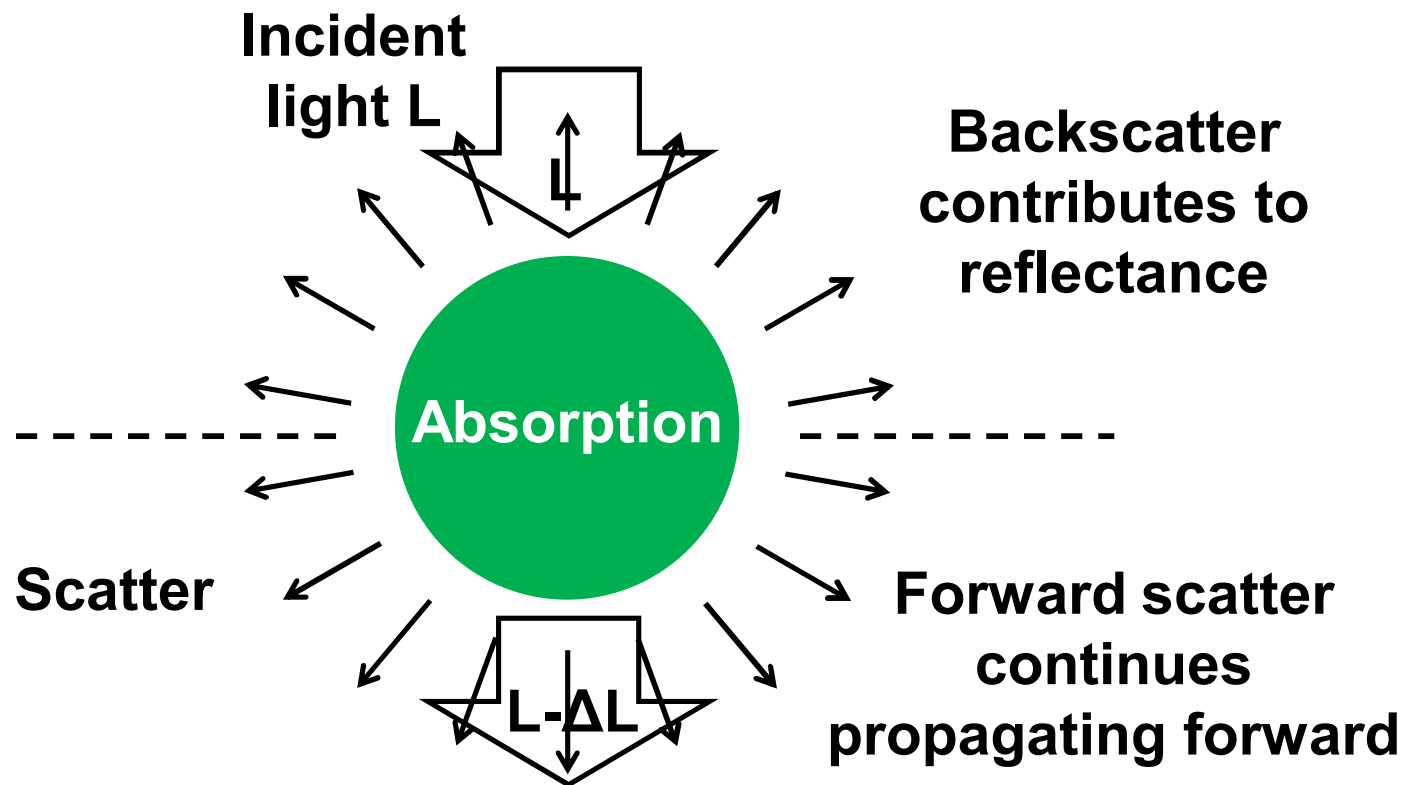




## Reflectance depends on single scattering albedo (u)

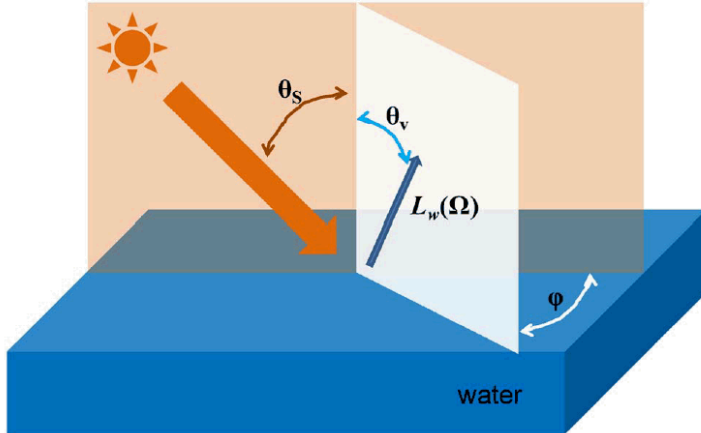
---

$$u(\lambda) = \frac{\text{Backscatter}(\lambda)}{\text{Backscatter}(\lambda) + \text{Absorption}(\lambda)} = \frac{b_b(\lambda)}{b_b(\lambda) + a(\lambda)}$$



# Reflectance Model of Z. Lee et al.

- Multiple scattering:  $r(\lambda) = G_1 u + G_2 u^2$



An inherent-optical-property-centered approach to correct the angular effects in water-leaving radiance

Zhong Ping Lee,<sup>1,\*</sup> Keping Du,<sup>2</sup> Kenneth J. Voss,<sup>3</sup> Giuseppe Zibordi,<sup>4</sup> Bertrand Lubac,<sup>5</sup> Robert Arnone,<sup>6</sup> and Alan Weidemann<sup>8</sup>

<sup>1</sup>Geosystems Research Institute, Mississippi State University, Stennis Space Center, Mississippi 39529, USA

<sup>2</sup>State Key Laboratory of Remote Sensing Science, Research Center for Remote Sensing and GIS, School of Geography, Beijing Normal University, Beijing, 100875, China

<sup>3</sup>Department of Physics, University of Miami, Coral Gables, Florida 33124, USA

<sup>4</sup>Global Environment Monitoring Unit, Joint Research Center, 21027 Ispra, Italy

<sup>5</sup>UMR-EPOC 5805, CNRS, Université de Bordeaux 1, Talence, 33405, France

<sup>6</sup>Naval Research Laboratory, Stennis Space Center, Mississippi 39529, USA

\*Corresponding author: zplee@nsl.msstate.edu

Received 12 January 2011; revised 29 March 2011; accepted 6 April 2011; posted 19 April 2011 (Doc. ID 141059); published 22 June 2011

Remote-sensing reflectance ( $R_m$ ), which is defined as the ratio of water-leaving radiance ( $L_w$ ) to downwelling irradiance [ $I_d(0^\circ)$ ], varies with both water constituents (including bottom properties of optically-shallow waters) and angular geometry.  $L_w$  is commonly measured in the field or by satellite sensors at convenient angles, while  $I_d(0^\circ)$  can be measured in the field or estimated based on atmospheric properties. To isolate the variations of  $R_m$  (or  $L_w$ ) resulting from a change of water constituents, effects of  $R_m$  (or  $L_w$ ) need to be removed. This is also a necessity for the calibration of remote-sensing instruments. The inherent-optical-property-centered approach is a system centered on water's inherent optical properties and offers an alternative to the

- $G_1$  and  $G_2$ 
  - Determined from numerical radiative transfer simulations
  - Validated with measurements

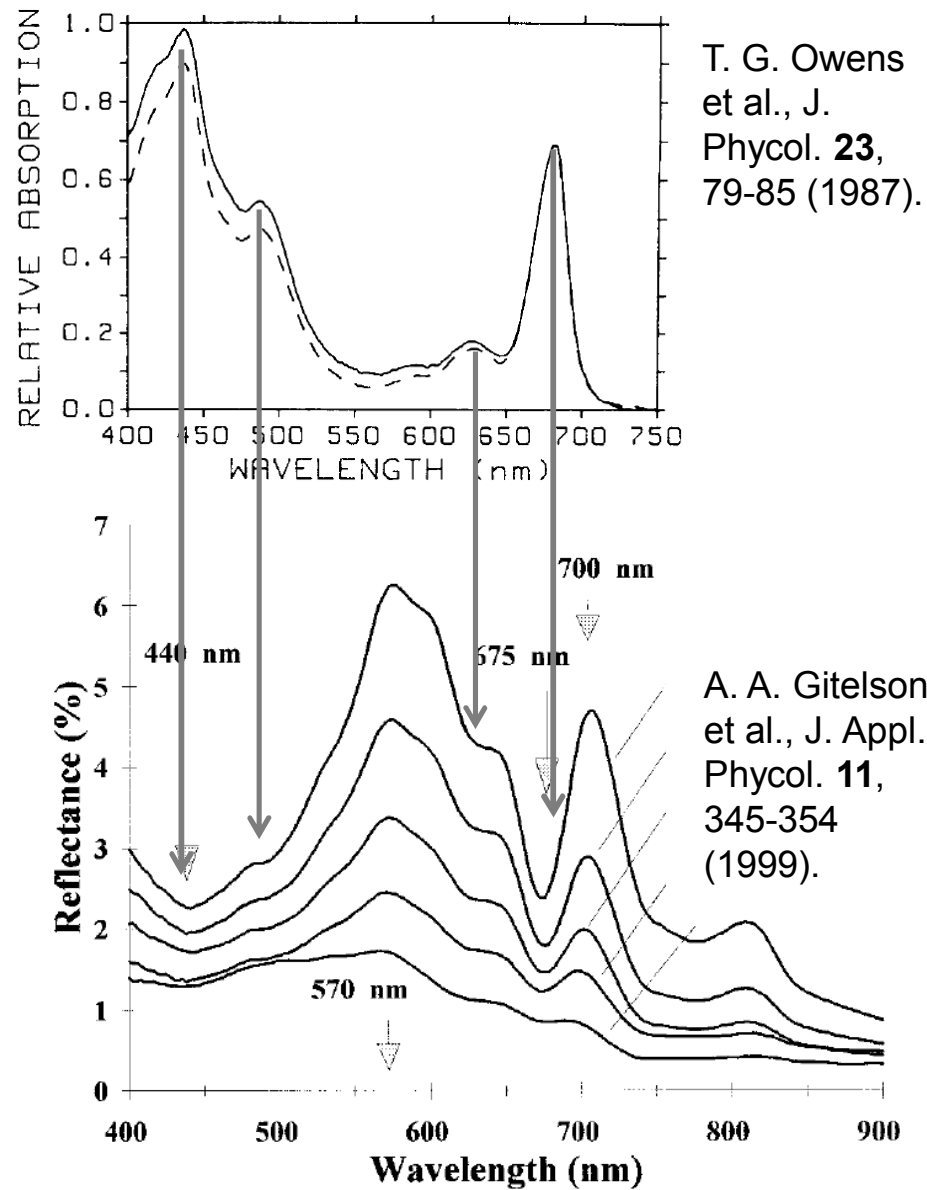
$$u(\lambda) = \frac{\text{Backscatter}(\lambda)}{\text{Backscatter}(\lambda) + \text{Absorption}(\lambda)} = \frac{b_b(\lambda)}{b_b(\lambda) + a(\lambda)}$$

# Reflectance $r(\lambda)$ : What is expected?

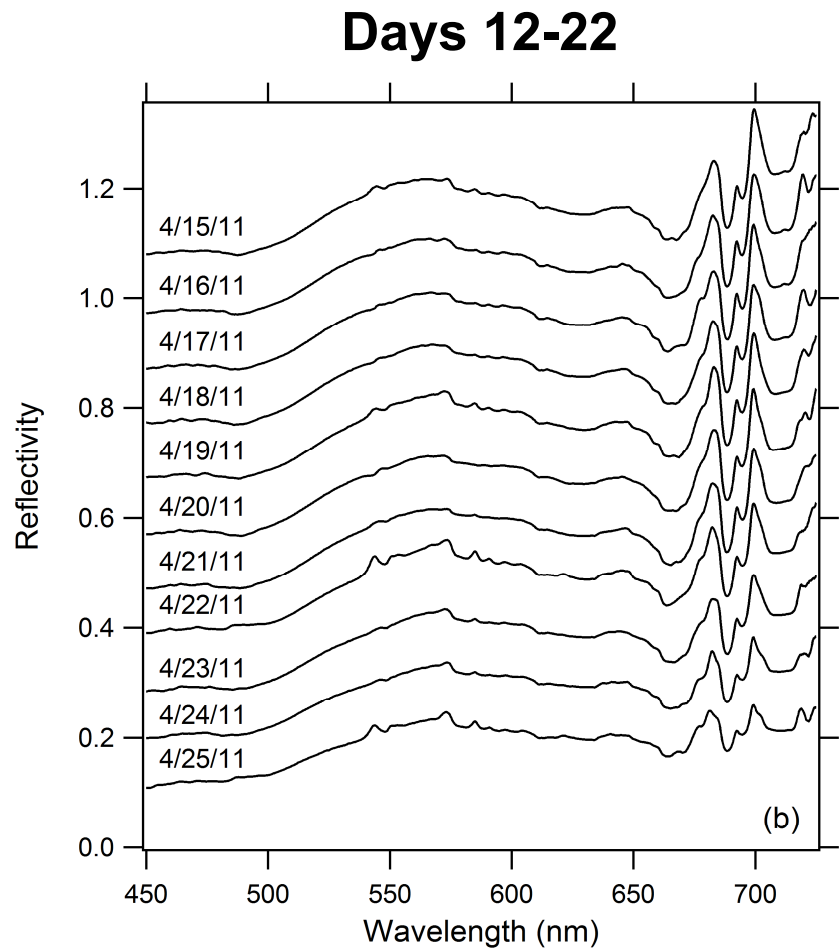
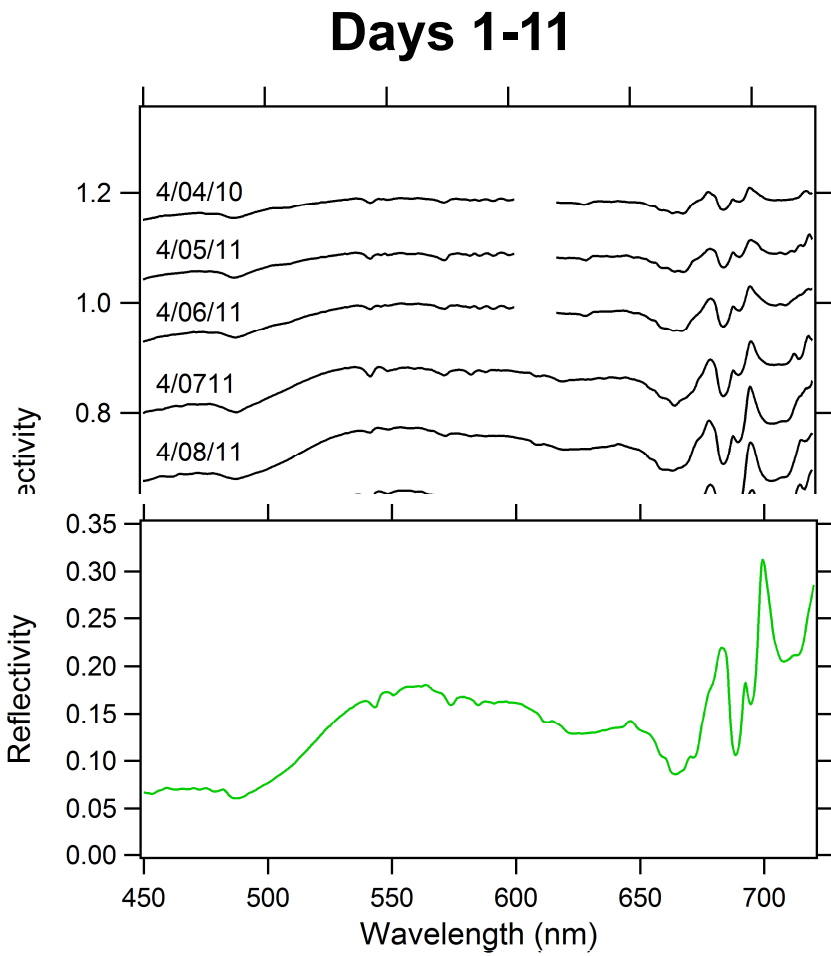
$$r(\lambda) \propto u(\lambda)$$

$$\propto \frac{b_b(\lambda)}{b_b(\lambda) + a(\lambda)}$$

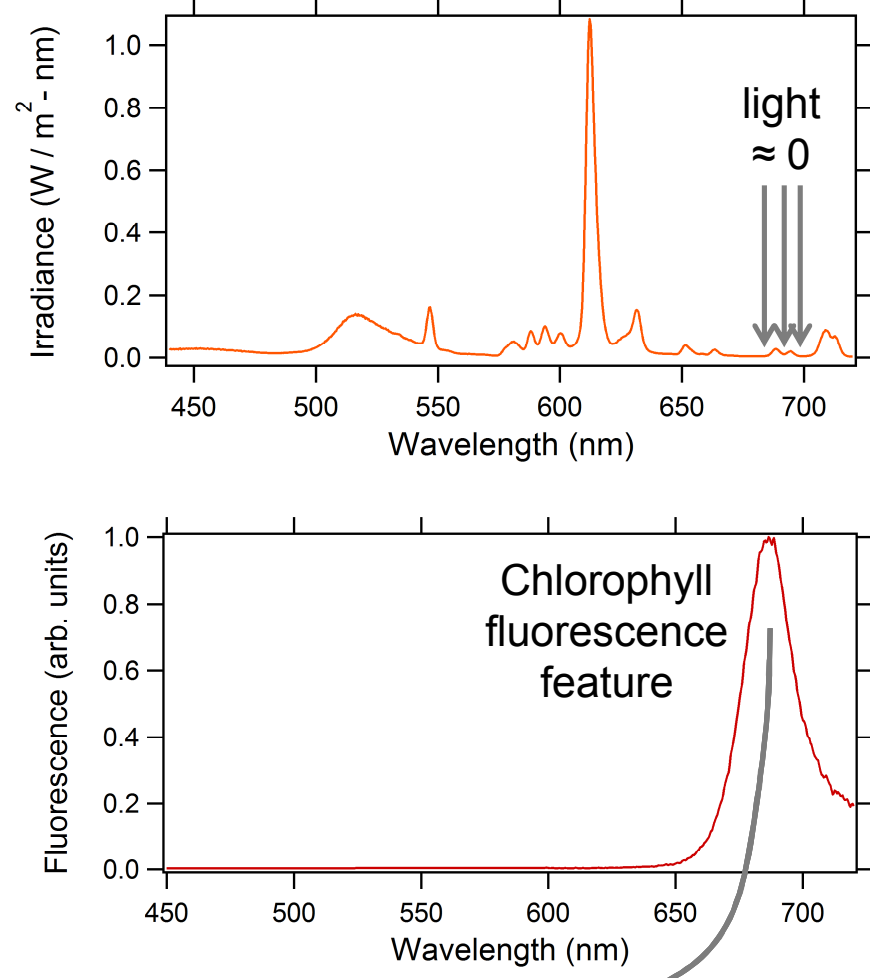
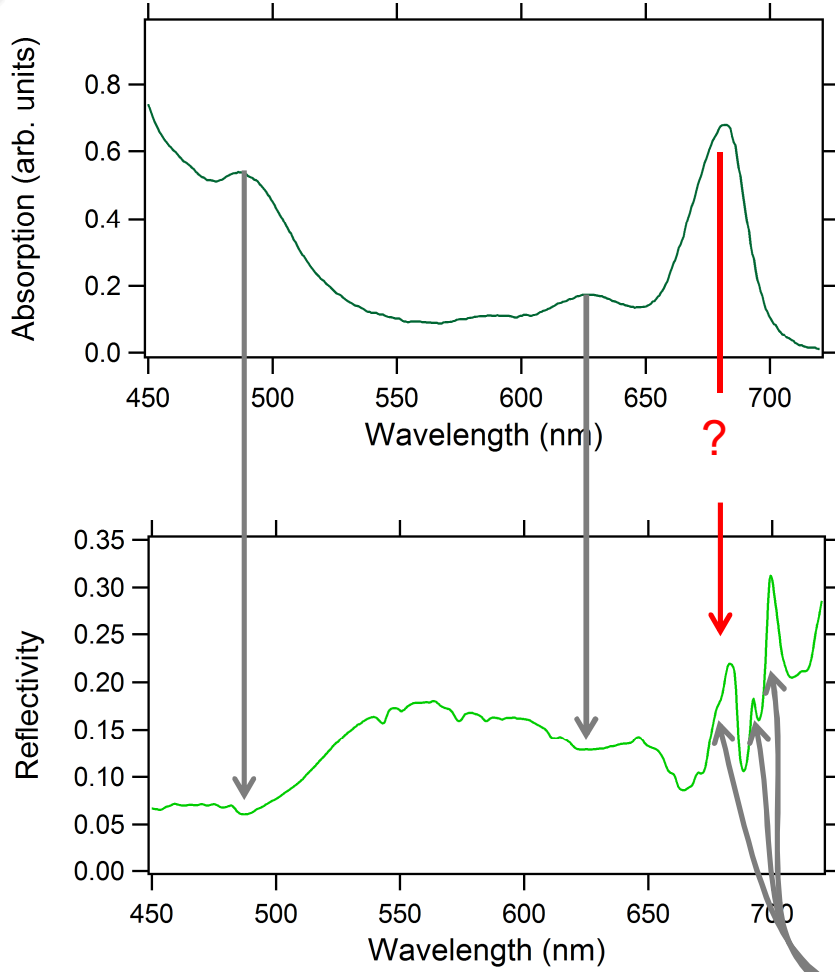
- $a(\lambda)$  is in the denominator
- Absorbance maxima should approximately correspond to reflectance minima
- More on this when we discuss the reflectance model



# Laboratory spectra (4/4/11 – 4/25/11)

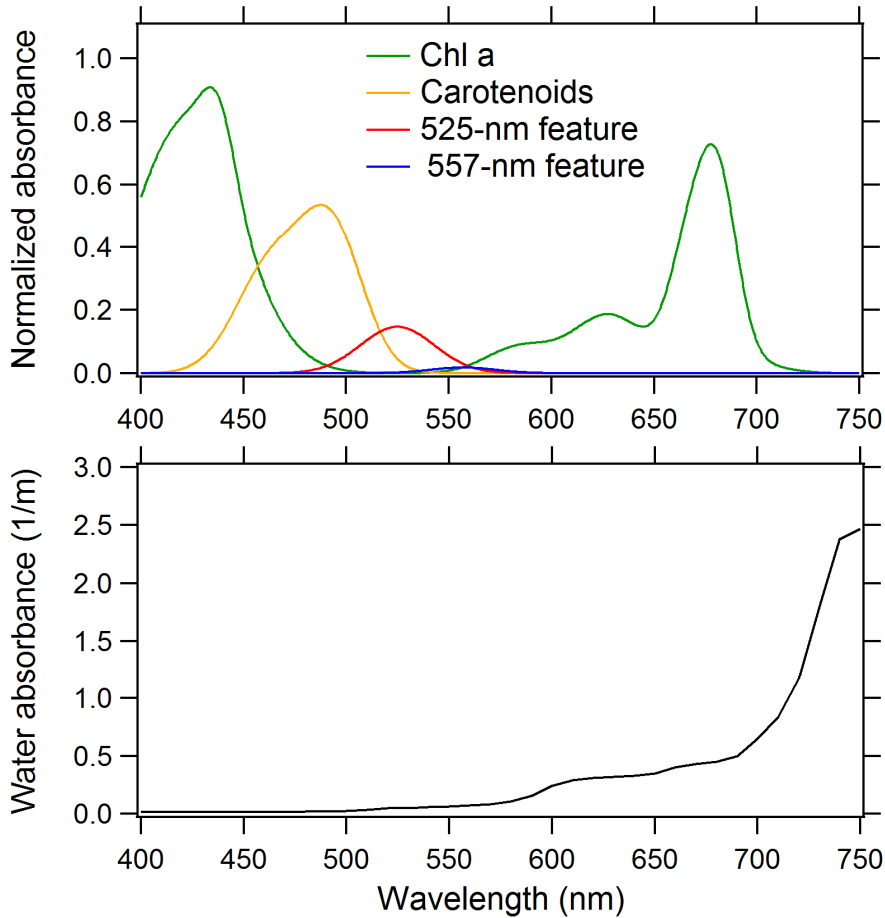


# Laboratory spectra (4/4/11 – 4/25/11)

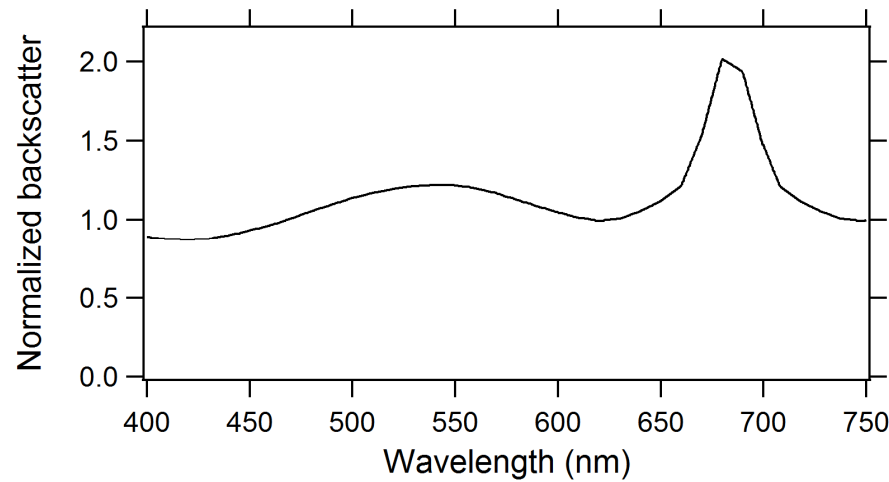


# This leaves only $a(\lambda)$ and $b_b(\lambda)$

$a(\lambda)$ : Algal pigments and water



$b_b(\lambda)$ : Generic phytoplankton backscattering spectrum from F. Lahet et al., *Remote Sens. Environ.* 72, 181-190 (2000).



# The unknowns of $r(\lambda)$

## Term in $r(\lambda)$

- $a(\lambda)$  = scaled sum of four components

Unknowns

$C_1, C_2, C_3, C_4$

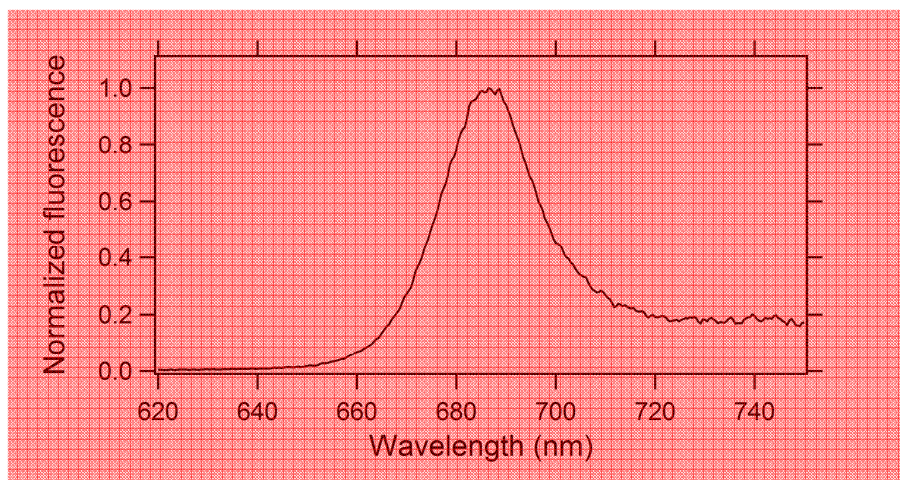
- $b_b(\lambda)$  = scaled phytoplankton backscatter spectrum

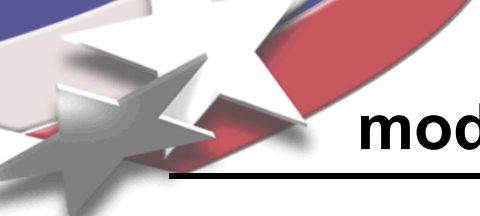
$C_5$

- Fluorescence = Scaled optically thin spectrum with re-absorption

$C_6, L_f$

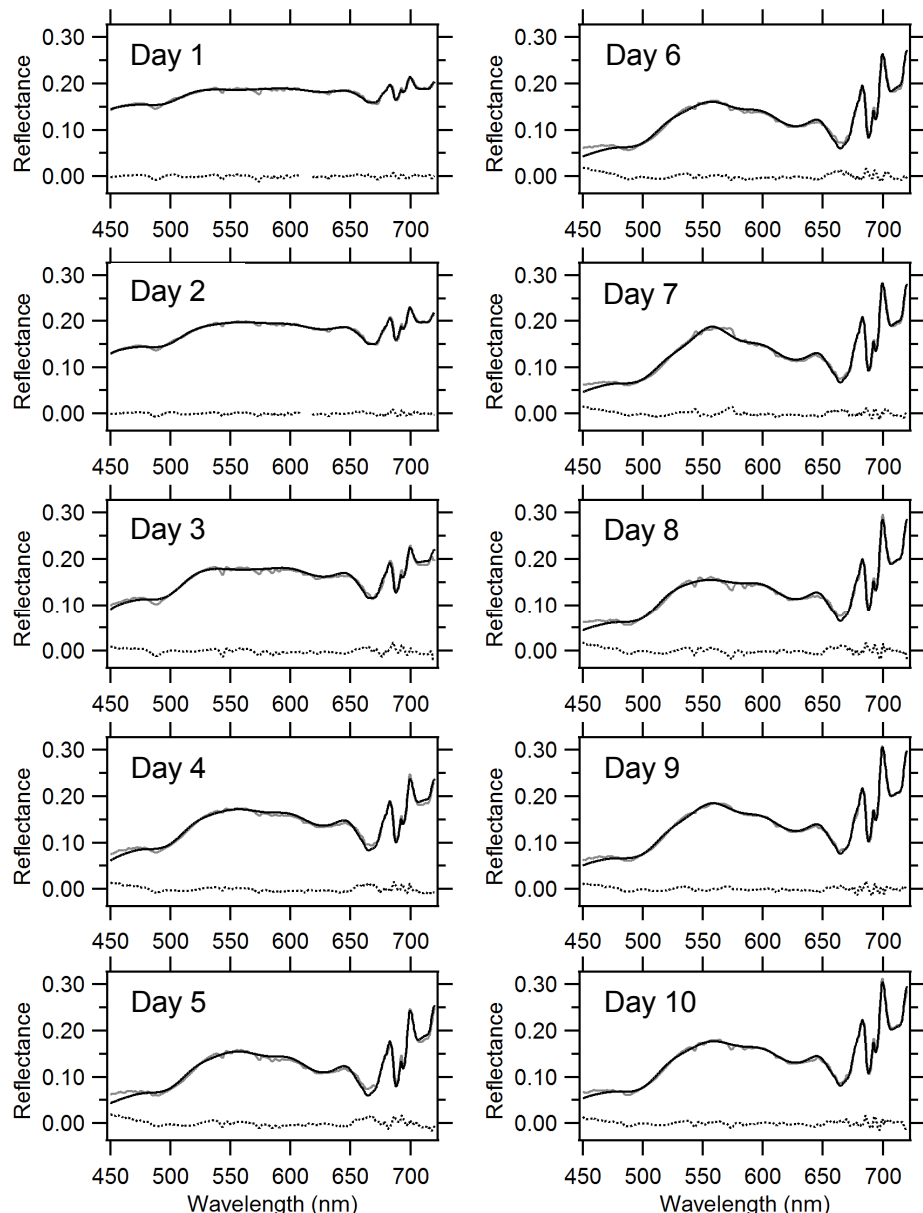
$$F = C_6 e^{F_{\text{tot}}} \exp(-\kappa L_f)$$





# Fitting the reflectance model to the reflectance measurements

- Displaying spectrum acquired 30 minutes after the lights were cycled on each day
- Values of  $C_1$ - $C_7$  are optimized to minimize the RMS error between the measurements and model
  - MATLAB's *fminsearch* routine
- Model captures the absorption and fluorescence features evident in data
- **Caution: 7 free parameters**



# Potential ambiguity accompanying our model inversion

K. Lumme, A. Penttilä / Journal of Quantitative Spectroscopy & Radiative Transfer 112 (2011) 1658–1670

1659

To interpret the polarimetric data the CB explanation is now universally accepted instead of some earlier semi empirical suggestions with full of various parameters. Although the mechanism itself is known, full scale fits to the data are still greatly underway. An obvious reason for the fact that the computations are so heavy that even modern computers cannot yet handle all of those, particularly true for the regoliths of the atmosphereless bodies which would require large model geometries to explain the opposition effect. The situation for the cometary aggregates for their polarization is easier because those are on the order of few tens of microns and due to their low density in the coma there are no multiple scattering effects.

Lasue et al. [7] and the references therein, fitted two cometary data sets of Halley and Hale-Bopp with a reasonable accuracy although the number of all kinds of free parameters in their model was rather excessive. The authors claim that the number is five, although there are a lot of hidden parameters which the authors assume to be known. Even with these parameters the authors are not satisfied with the fits at small phase angles. The old phrase goes: "give me seven free parameters and I can fit an elephant". A reasonable method to study the sensitivity of the derived parameters for a model in a case of a good data set would be to use only some parts of the whole set and check how well the model predicts the other parts. The more the parameters used in a model, the more sensitive will the fit be to the other parts.

Unfortunately there are no recent articles concerning CB fits to the large amount of observational data of the brightness behavior of the atmosphereless bodies. Therefore, no quantitative results exist for the opposition effect. Known to be the correct explanation CB still remains without exact proofs for that part. In this spirit a new semi-analytical approach was suggested by Muinonen [8,18] who showed that the combination of the classical ray tracing radiative transfer formalism with the CB formalism explains nicely the exact superposition  $T$ -matrix method (CTm) [9] results in small geometries. Extension of this to very large geometries also seems to explain the extremely sharp opposition effect.

## 2. Structure and morphology of cometary and regolith dust

What will follow we assume that all the constituent particles (monomers) have a touching neighbor. This applies both to the aggregates and regolith models. If this is not the case we would have a cloud of particles. The requirement need not be actually quite true because some electrostatic forces can produce some separation. Our computations have shown, however, that if the separation of two monomers is less than about 10% of the radii the results are fairly insensitive to that assumption.

### 2.1. Cometary and regolith dust

Altogether we will assume two kinds of monomer shapes: spheres and Gaussian random spheres (GRS). We also have an efficient code for the packing of general

ellipsoids of varying sizes. We do not accept the state-

satisfied with the fits at small phase angles. The old phrase goes: "give me seven free parameters and I can fit an elephant". A reasonable method to study the

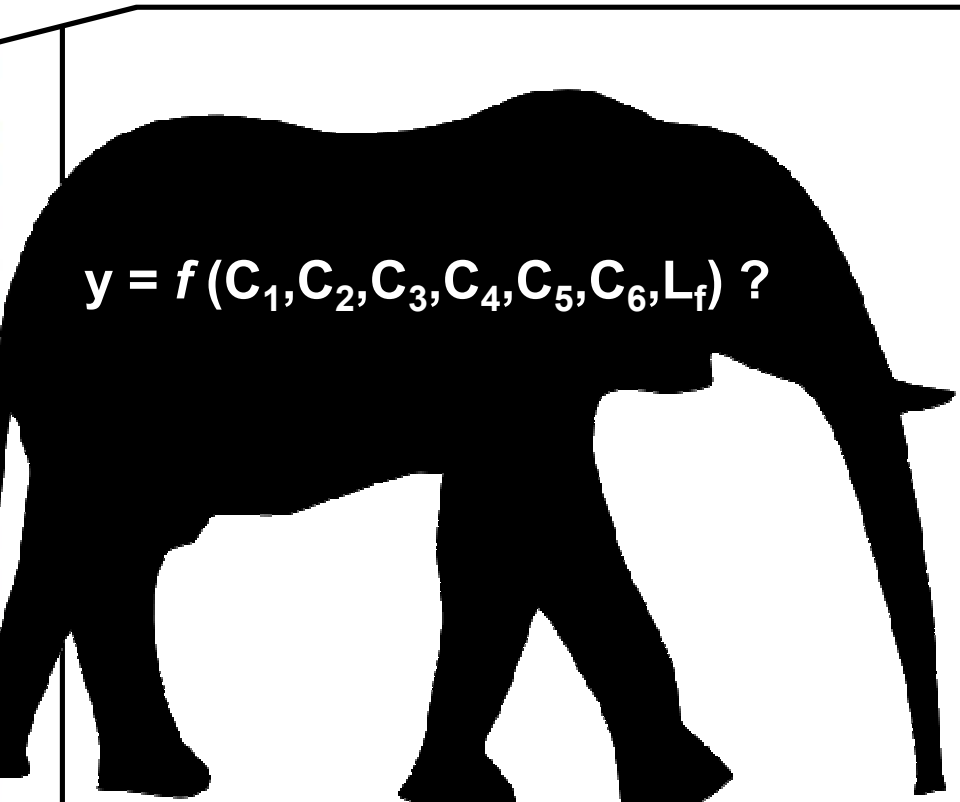
We have used size distributions which included scale breaks. The dimensions of the monomers are neither spherical nor ellipsoidal and they seem to have two size scales. The radii of the monomers are typically in the range  $0.05 < r < 0.25 \mu\text{m}$  and the diameters of the aggregates  $\sim 20 \mu\text{m}$ . These values are also in accordance with those of Hanner and Bradley [10]. Some of them resemble a particle-cluster aggregate (PC) while the others are closer to a cluster-cluster aggregate (CC). The terms often used for these are fractal and/or fluffy aggregates. This terminology is not very accurate because either the possible fractal structure or the fluffiness cannot be deduced reliably from the 2D images.

In building our PC packings we have used two different schemes. The first one assumes ballistic linear trajectories from random directions for a new monomer and sticking to the aggregate when meeting any of the existing ones. This first scheme produces aggregates almost always with roughly the same packing density. Our second aggregate building scheme tries to put a new monomer next to the existing ones so close/far from the aggregate center (the position of the first monomer) as possible. By this way we can vary the resulting packing density of the aggregate. The selection of the position of a new monomer is based on the binomial distribution statistics. In the CC packings we build certain number of sub-PC aggregates separately and let them collide with the others at a single point.

For the size distribution of the monomers we have tried two different statistics: power law and lognormal distribution. In the case of the power law we used different exponents in the range  $2.75 < \gamma < 3.25$  and for the lower and upper limits of the cut-off radii  $0.05$  and  $0.25 \mu\text{m}$ . For the lognormal distribution we have assumed that 98% of the monomers are in the interval given above. In the final light scattering results we cannot see very much difference between the two choices of the distributions. Our existing light scattering codes put an upper limit to the number of monomers to  $n \sim 2000$ . Fortunately the results are not too sensitive to  $n$  when  $n > \sim 250$ .

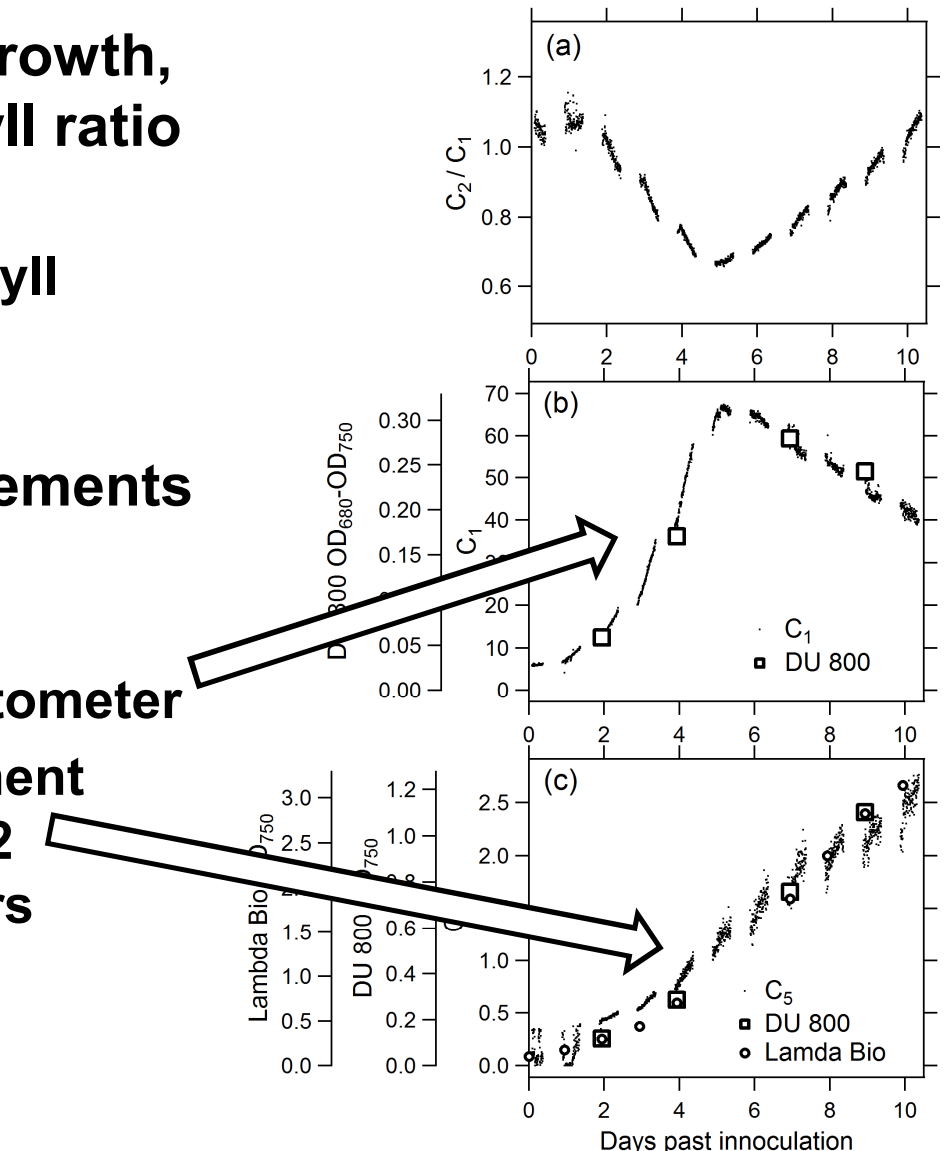
An important quantity related to the structure of the aggregate is the packing or volume density which we shall denote by  $p_d$ , which is equal to one minus porosity. Several reference geometries have been suggested to estimate the volume which encompasses the whole aggregate. In the past the standard geometry was a sphere which for the elongated aggregates can largely exaggerate

$$y = f(C_1, C_2, C_3, C_4, C_5, C_6, L_f) ?$$



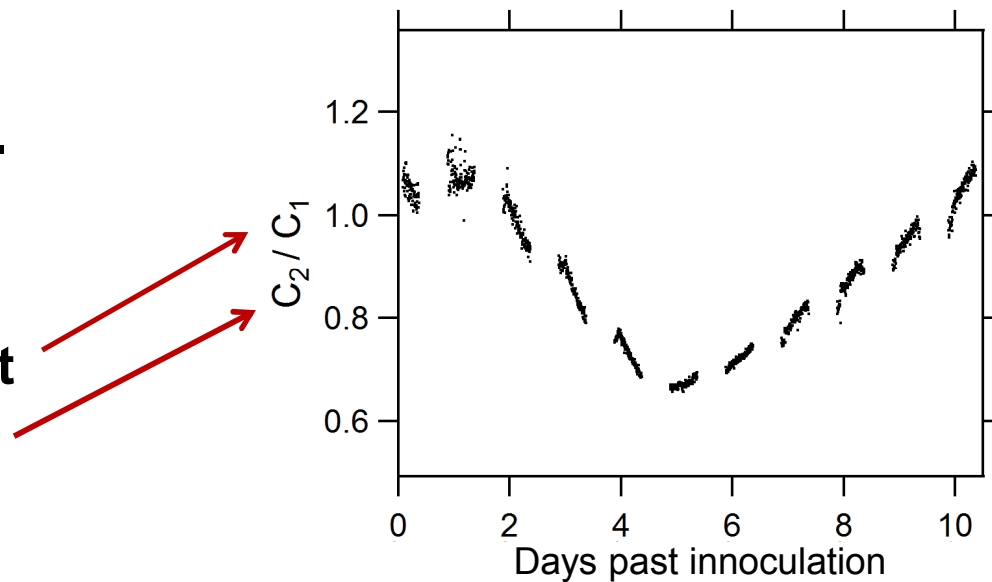
# Comparison to expectations (and offline sampling measurements)

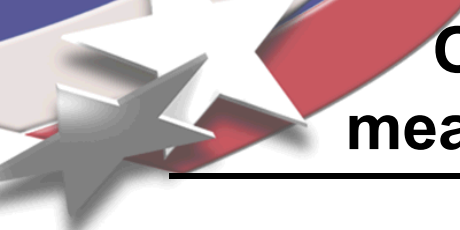
- During exponential-phase growth, the carotenoid-to-chlorophyll ratio decreases
  - Expected because chlorophyll plays a more central role in photosynthesis
- Spectrophotometer measurements conducted on grab samples
  - Chl-a coefficient in good agreement with spectrophotometer
  - Backscatter in good agreement with OD750 measured with 2 different spectrophotometers



# Acknowledging the elephant: Comparison to expectations and sampling

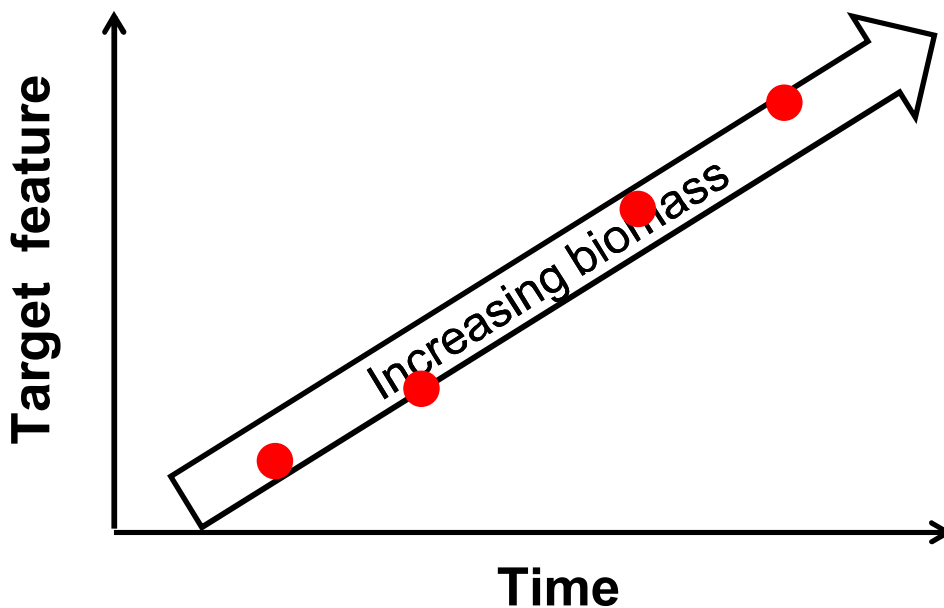
- During exponential-phase growth, the carotenoid-to-chlorophyll ratio decreases
  - $C_1$ : Chlorophyll coefficient
  - $C_2$ : Carotenoid coefficient
  - Trend expected: Chlorophyll more central in photosynthesis



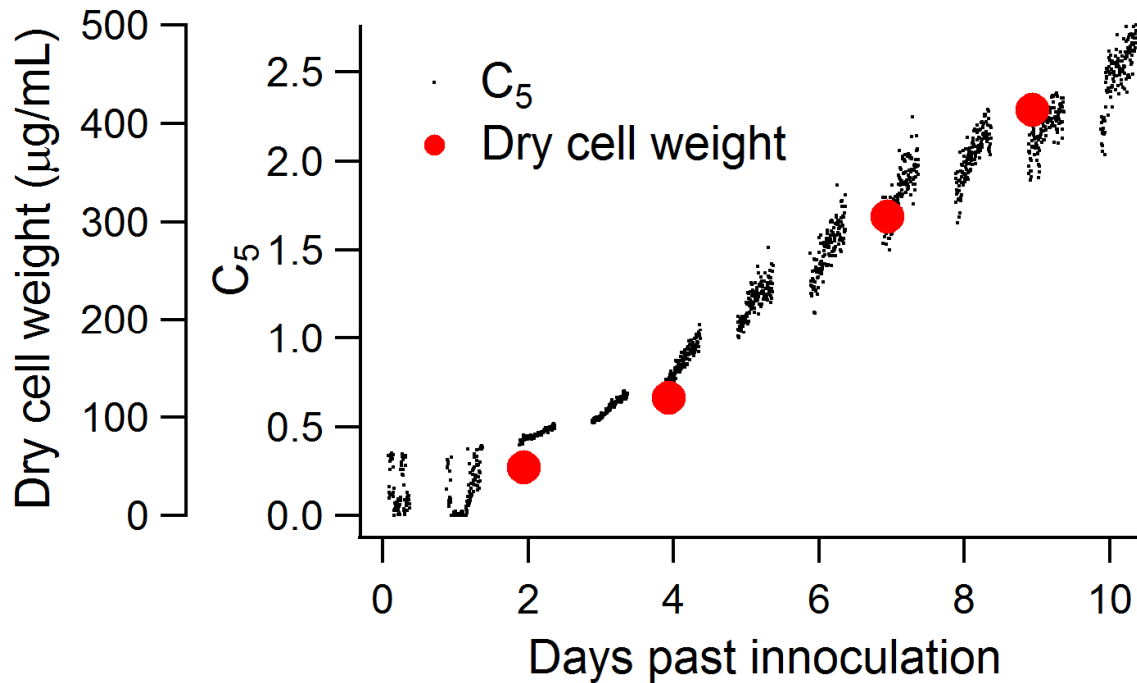


# Original question: Can biomass be measured without sampling the culture?

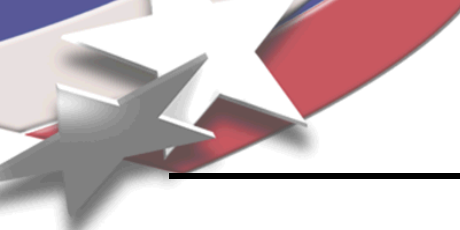
---



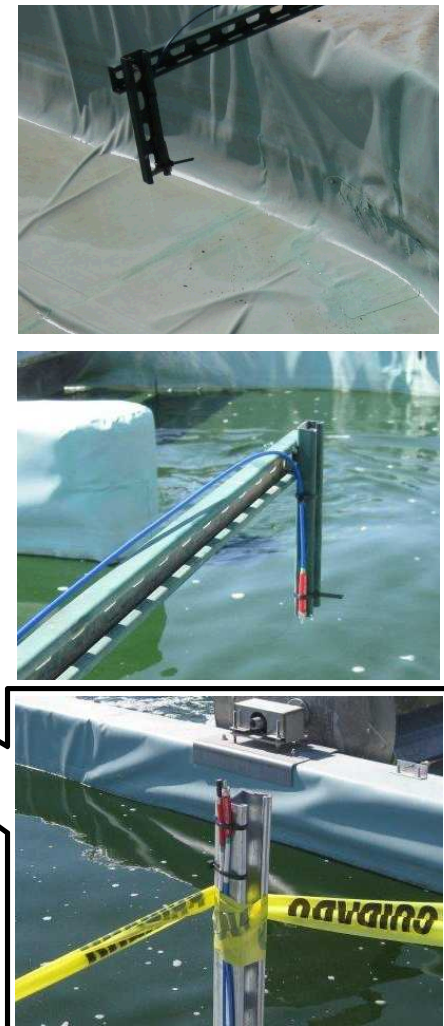
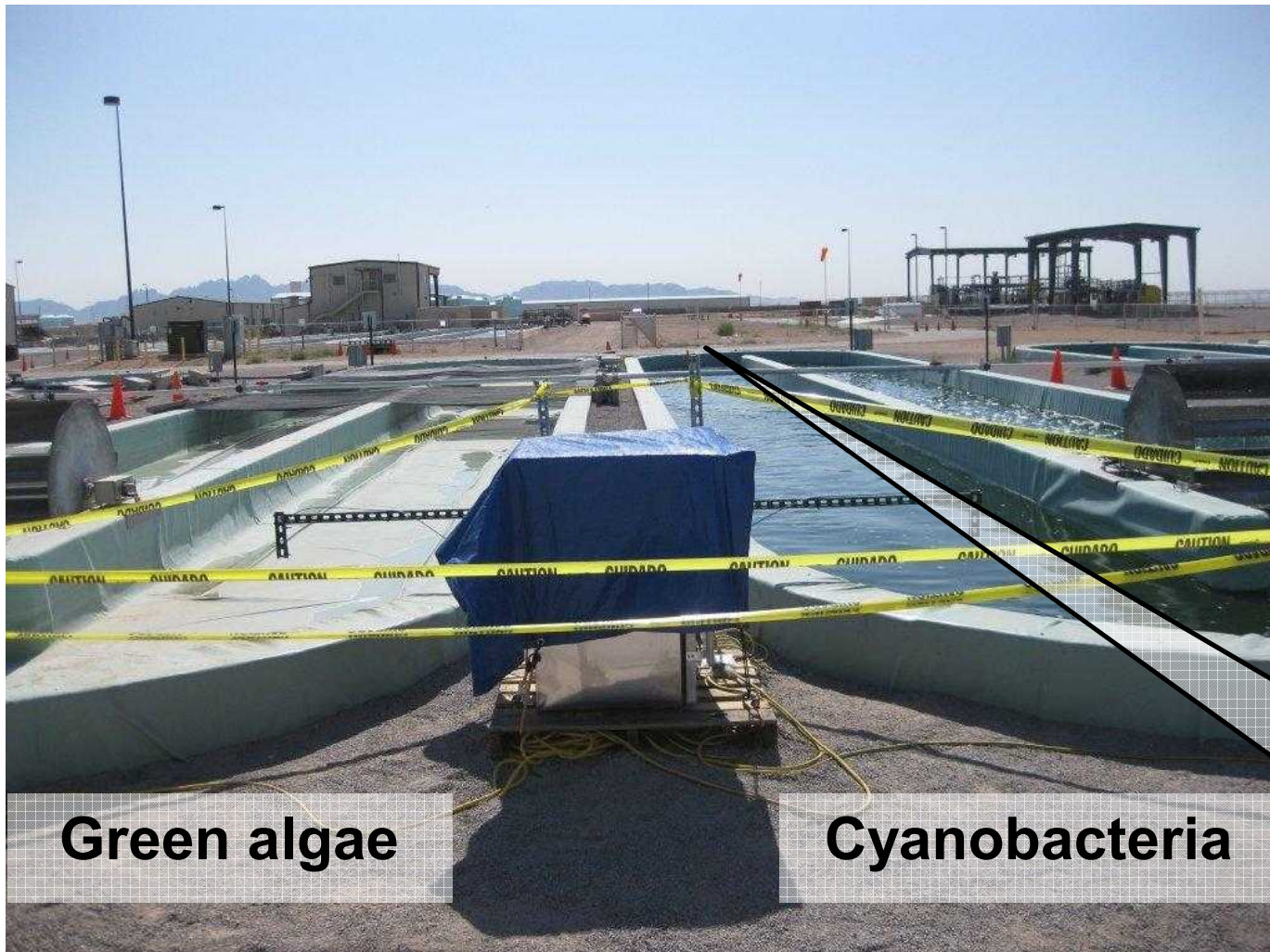
# Original question: Can biomass be measured without sampling the culture?

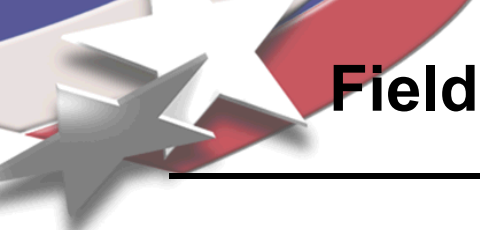


- Answer: Yes – the algal backscatter coefficient scales with algal dry cell weight.
- Also, pigment absorption and fluorescence provide information on algal health and state-of-growth



# Deployed at Sapphire Energy (Las Cruces, NM)





# Field Deployment Brings New Challenges

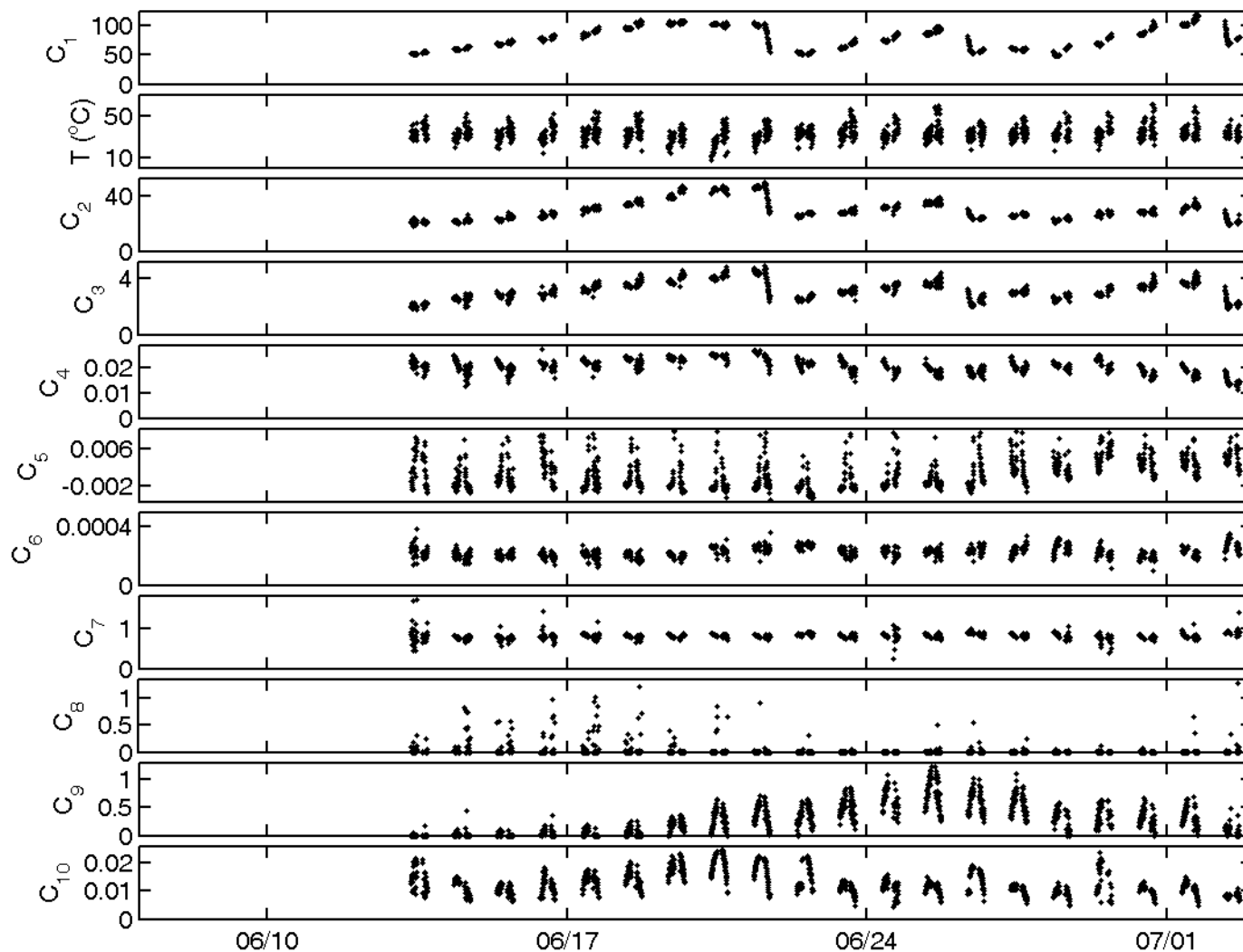
---

- 1) Need a backscattering spectrum specific to the algal species
- 2) Need to account for variable position of the sun
- 3) Need to account for different downwelling light fields from the sun (direct) and sky (diffuse)
- 4) Need to account for shadows and variable clouds

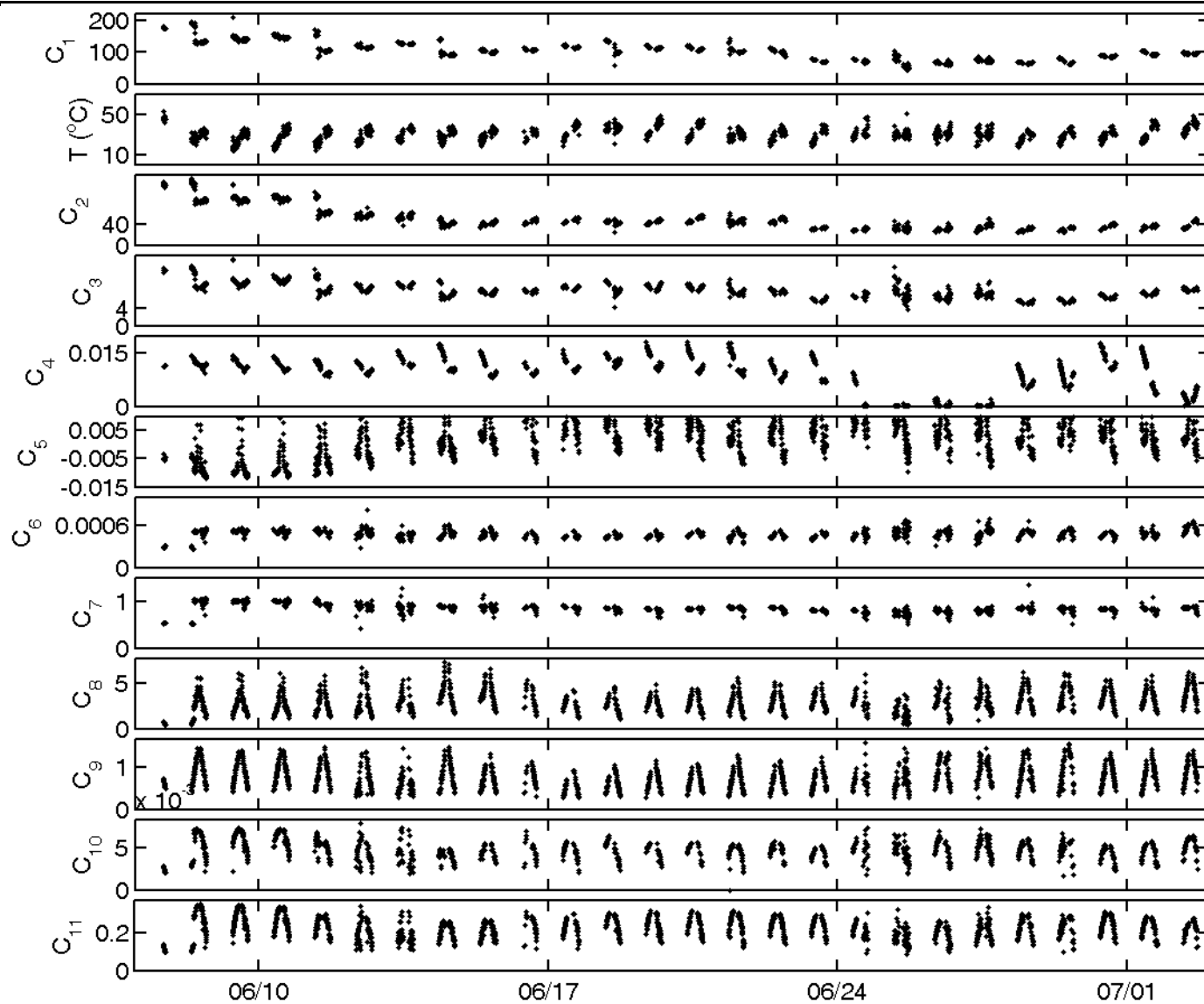
  

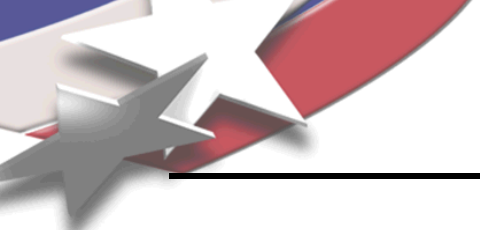
- Each challenge is expected to add  $\geq 1$  terms to the reflectance model.

# Fitting Parameters for Green Algal Culture



# Fitting Parameters for Cyanobacterial Culture





# Summary

---

- ***In-situ* measurement of biomass and pigment optical activity**
  - **Extremely rapid (~5-min) measurement times**
- **Non-sampling**
  - **No laboratory access required**
- **Integrates rigorous light transport physics into the data analysis**
  - **No extensive pre-calibration required**
- **Non-contact**
  - **Avoids instrument fouling**
- **Fully autonomous operation**
  - **Deployed over several months in the field**

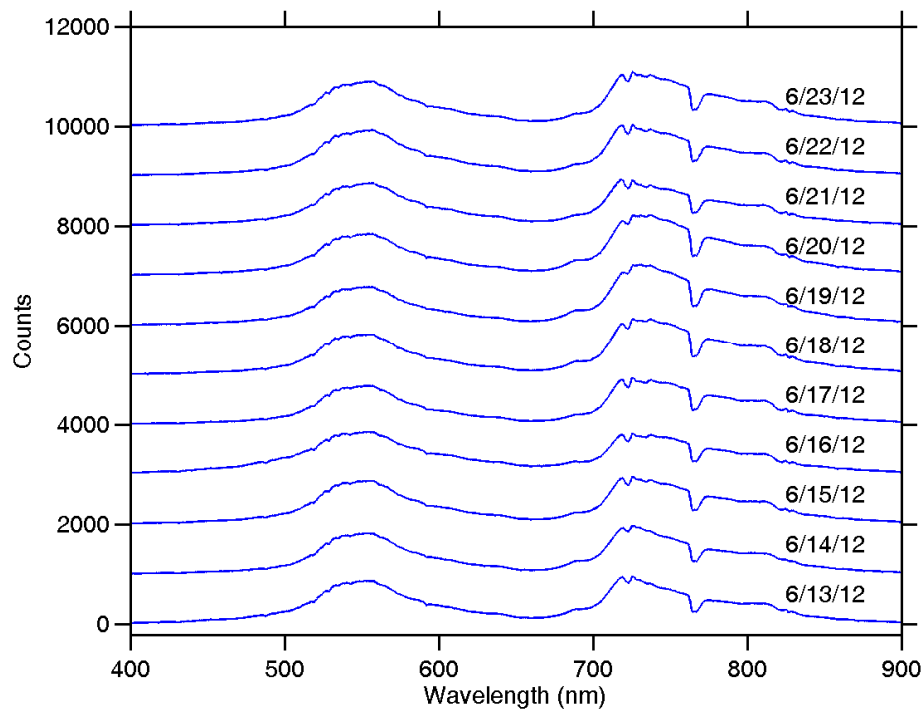


---

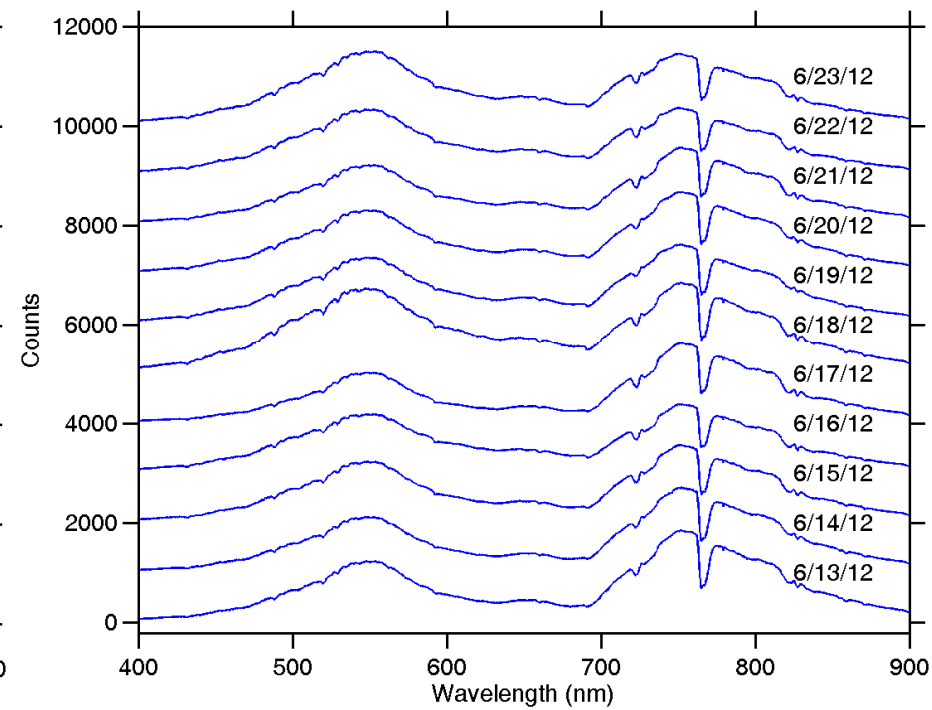
# Backup Slide deck

# Example data acquired at ~8:30 AM

**Green algae**

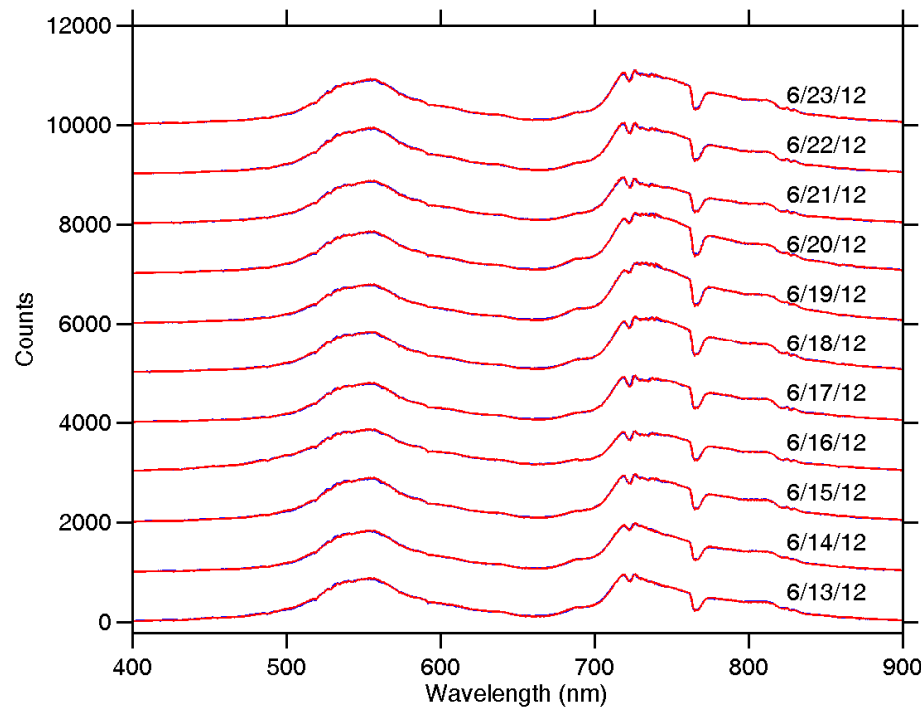


**Cyanobacteria**

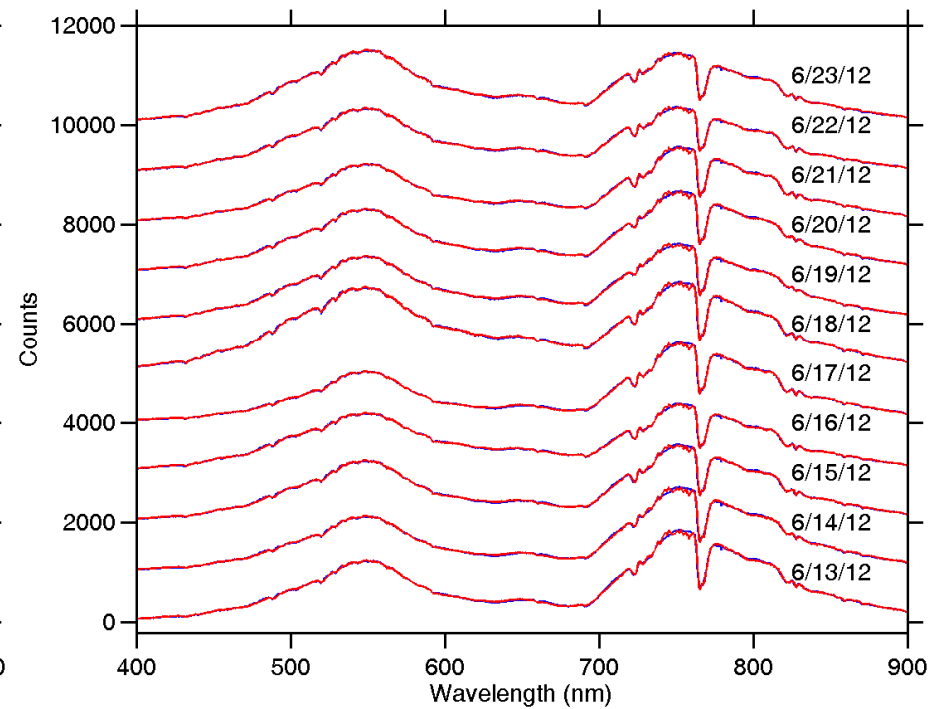


# Example fitting results

**Green algae**



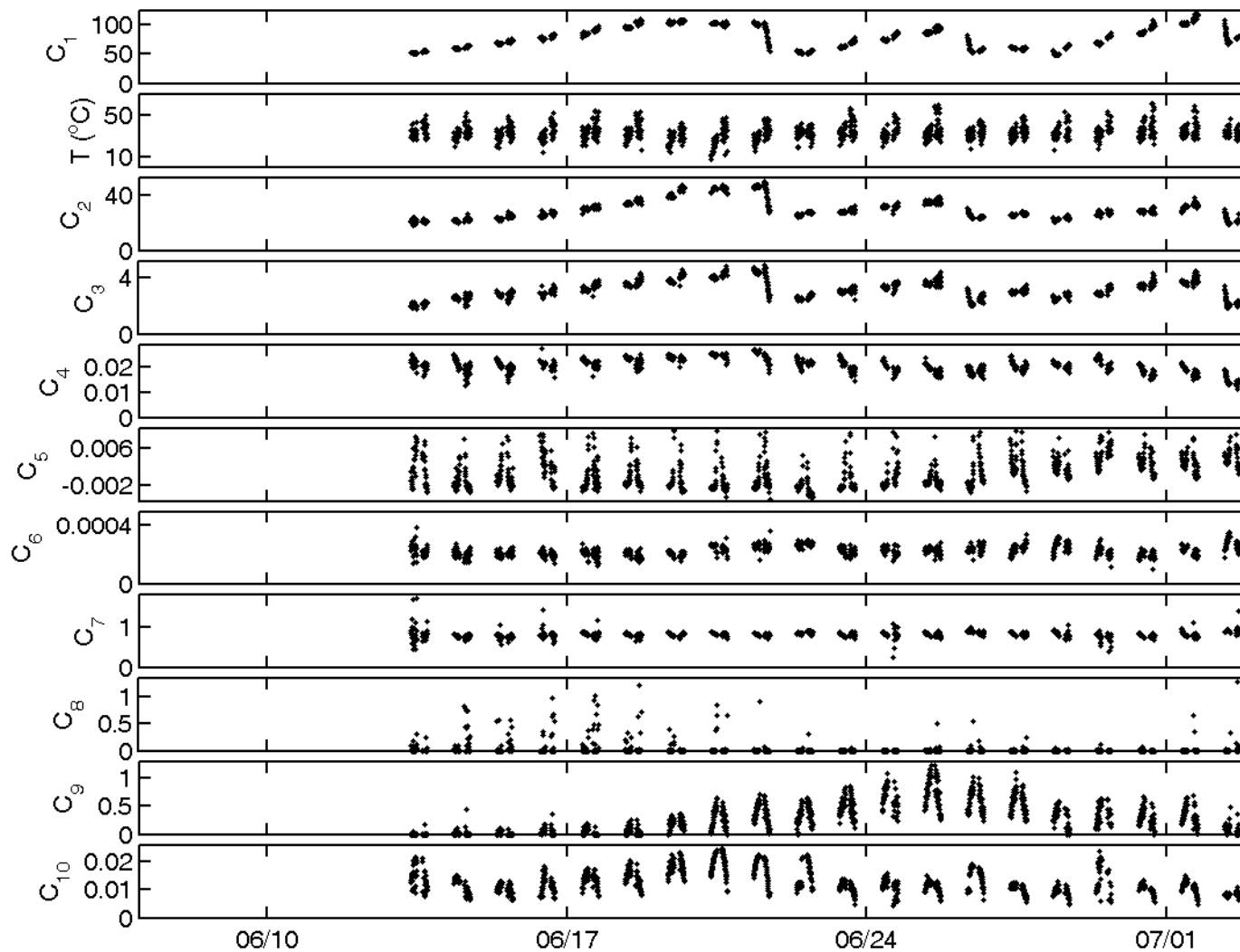
**Cyanobacteria**



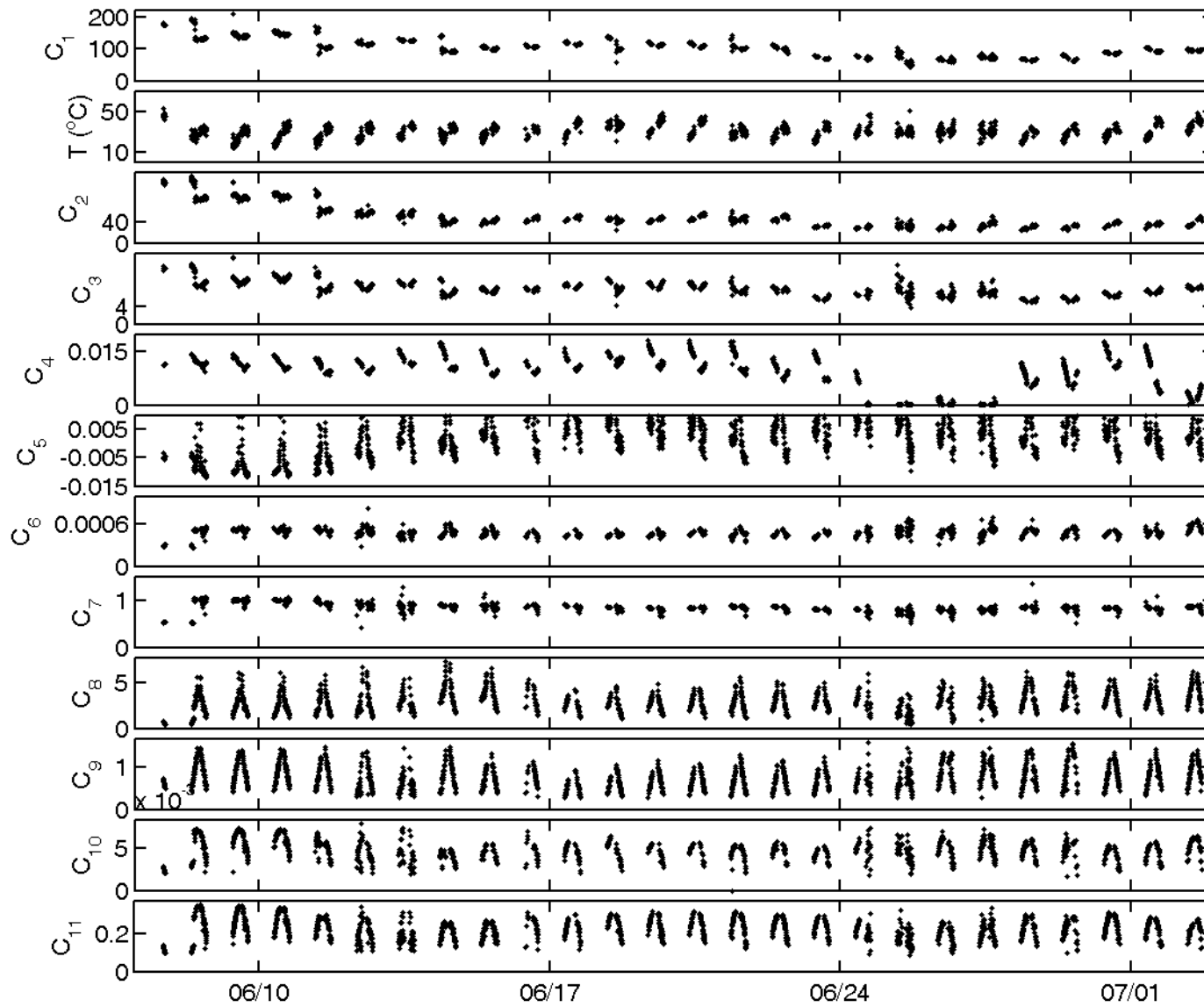
**11 fitting parameters**

**12 fitting parameters**

# Fitting Parameters for Green Algal Culture



# Fitting Parameters for Cyanobacterial Culture



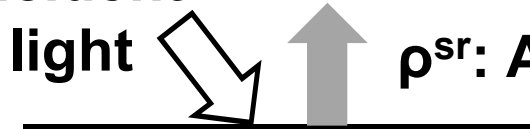


# Shallow-water reflectance model

## Lee et al., U. of S. Florida (1998,1999)

---

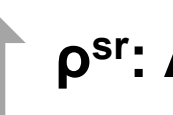
Incident

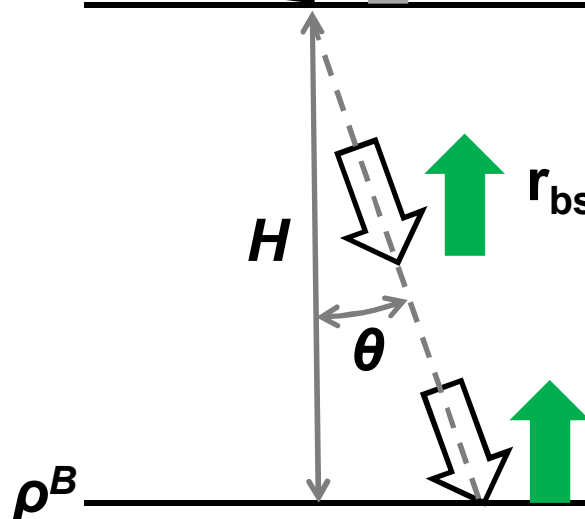


Multiple scatter results in two effects:

- (1) Increased angular spreading of light field
- (2) Higher-order dependence on scatter:  $r(\lambda) \propto [u(\lambda)]^n$ ,  $n > 1$

Incident

light   $\rho^{sr}$ : Above-surface specular reflectance 



$r_{bs}^C$ : Below-surface volumetric reflectance  
from water column

$r_{bs}^B$ : Below-surface reflectance from  
bottom

Multiple scatter results in two effects:

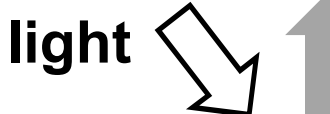
- (1) Increased angular spreading of light field
- (2) Higher-order dependence on scatter:  $r(\lambda) \propto [u(\lambda)]^n$ ,  $n > 1$



# Shallow-water reflectance model

## Lee et al., U. of S. Florida (1998,1999)

Incident



$\rho^{sr}$ : Above-surface specular reflectance

Diagram illustrating light scattering in shallow water. A vertical line represents the water column of height  $H$ . Incident light (grey arrow) hits the surface. A green arrow represents the scattered light. The angle of incidence is  $\theta$ .

Equations for above-surface specular reflectance:

$$r_{bs}^{dp} = (g_0 + g_1 u^{g_2}) u \quad \text{Higher-order dependence on } u$$

$$r_{bs}^C = r_{bs}^{dp} \left( 1 - \alpha_0 \exp \left\{ - \left[ \frac{1}{\cos(\theta)} + D_0 (1 + D_1 u)^{0.5} \right] \kappa H \right\} \right)$$

Angular spreading is indicated by the red bracket under the term  $(1 + D_1 u)^{0.5}$ .

$$\kappa = a + b_b$$

$$r_{bs}^B = \alpha_1 \rho^B \exp \left( - \left[ \frac{1}{\cos(\theta)} + D_0' (1 + D_1' u)^{0.5} \right] \kappa H \right)$$

Angular spreading is indicated by the red bracket under the term  $(1 + D_1' u)^{0.5}$ .

Multiple scatter results in two effects:

- (1) Increased angular spreading of light field
- (2) Higher-order dependence on scatter:  $r(\lambda) \propto [u(\lambda)]^n$ ,  $n > 1$

# Shallow-water reflectance model

## Lee et al., U. of S. Florida (1998,1999)

Incident



$\rho^{sr}$

Above-surface specular reflectance

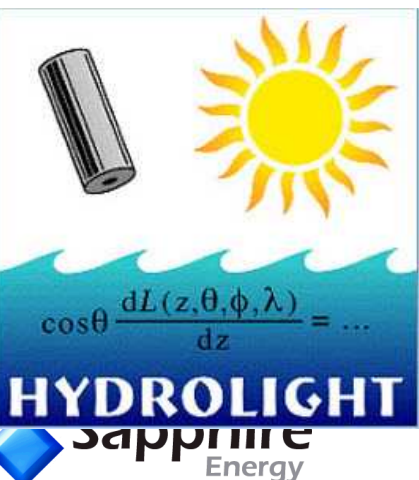
$$r_{bs}^{dp} = (g_0 + g_1 u^{g_2}) u \quad \text{Higher-order dependence on } u$$

$$r_{bs}^C = r_{bs}^{dp} \left( 1 - \alpha_0 \exp \left\{ - \left[ \frac{1}{\cos(\theta)} + D_0 (1 + D_1 u)^{0.5} \right] \kappa H \right\} \right)$$

Angular spreading

$$\kappa = a + b_b$$

$$r_{bs}^B = \alpha_1 \rho^B \exp \left( - \left[ \frac{1}{\cos(\theta)} + D_0' (1 + D_1' u)^{0.5} \right] \kappa H \right)$$



- Lee et al. ran radiative transfer simulations to provide values for 9 of these parameters
  - $g_0, g_1, g_2, \alpha_0, \alpha_1, D_0, D_1, D_0', D_1'$
- $H, \theta, \rho^B$ , and  $\rho^{sr}$  can be measured.